

Some Numerical Techniques for Maxwell's Equations in Different Types of Geometries

Bengt Fornberg*

University of Colorado, Department of Applied Mathematics, 526 UCB, Boulder, CO 80309, USA (fornberg@colorado.edu)

Summary. Almost all the difficulties that arise in finite difference time domain solutions of Maxwell's equations are due to material interfaces (to which we include objects such as antennas, wires, etc.) Different types of difficulties arise if the geometrical features are much larger than or much smaller than a typical wave length. In the former case, the main difficulty has to do with the spatial discretization, which needs to combine good geometrical flexibility with a relatively high order of accuracy. After discussing some options for this situation, we focus on the latter case. The main problem here is to find a time stepping method which combines a very low cost per time step with unconditional stability. The first such method was introduced in 1999 and is based on the ADI principle. We will here discuss that method and some subsequent developments in this area.

Key words: Maxwell's equations, FDTD, ADI, split step, pseudospectral methods, finite differences, spectral elements.

1 Introduction

The main difficulties that arise when solving Maxwell's equations with finite differences usually come from the (often irregular) shapes of material interfaces. There are two different length scales present in CEM (computational electromagnetics) problems:

- the size of geometrical features, and
- a typical wave length.

In many problems the two length scales are of comparable size. The (partly conflicting) goals that then need to be met by an effective numerical method include:

- good geometric flexibility (to allow for interfaces with corners or with high curvatures);
- high order of spatial accuracy (to keep the number of points per wavelength low);
- guaranteed (conditional) time stepping stability; and

* The work was supported by NSF grants DMS-0073048, DMS-9810751 (VIGRE), and also by a Faculty Fellowship from the University of Colorado at Boulder.

– low computational cost.

There are also many important applications in which the first length scale (the size of geometrical features) is far smaller than a typical wave length – maybe by five orders of magnitude, or more. Examples of such situations include the interactions between components on an integrated circuit, the effect of cellular phone signals on brain cells, and those of a lightning strike on an aircraft. In order to capture the geometry, we then need to use grids which (at least in some areas) feature an extremely high number of points per wavelength (PPW). High formal order of accuracy in the spatial discretization is then less critical. On the other hand, the method to advance in time should feature:

- explicit (or effectively explicit) time stepping (since grids tend to be extremely large); and
- the complete absence of any CFL-type stability condition (since such conditions would force time step sizes many orders of magnitude smaller than what is needed in order to accurately resolve the wave).

The first time stepping method that met both these criteria was introduced in 1999 [46]. Since then, a second (different, but related) method has been proposed [29]. Furthermore, both of these methods have been enhanced to feature higher than second order of accuracy in time [30]. As their only nontrivial step, they both require the solution of tridiagonal linear systems. One of the approaches is based on the alternating direction implicit method (ADI), and the other one on a split step (SS) concept.

In this article, we will first state the 3D Maxwell’s equations (formulated in 1873 by James Clark Maxwell, [32]), and then summarize the classical Yee scheme [44]. Following that, we will discuss the issues that have been mentioned above. The main focus of this review will be on fast and unconditionally stable time stepping procedures.

2 Maxwell’s Equations and the Yee Scheme

Assuming no free charges or currents, the 3D Maxwell’s equations can be written

$$\left\{ \begin{array}{l} \frac{\partial E_x}{\partial t} = \frac{1}{\varepsilon} \left(\frac{\partial H_z}{\partial y} - \frac{\partial H_y}{\partial z} \right) \\ \frac{\partial E_y}{\partial t} = \frac{1}{\varepsilon} \left(\frac{\partial H_x}{\partial z} - \frac{\partial H_z}{\partial x} \right) \\ \frac{\partial E_z}{\partial t} = \frac{1}{\varepsilon} \left(\frac{\partial H_y}{\partial x} - \frac{\partial H_x}{\partial y} \right) \end{array} \right. \quad \left\{ \begin{array}{l} \frac{\partial H_x}{\partial t} = \frac{-1}{\mu} \left(\frac{\partial E_z}{\partial y} - \frac{\partial E_y}{\partial z} \right) \\ \frac{\partial H_y}{\partial t} = \frac{-1}{\mu} \left(\frac{\partial E_x}{\partial z} - \frac{\partial E_z}{\partial x} \right) \\ \frac{\partial H_z}{\partial t} = \frac{-1}{\mu} \left(\frac{\partial E_y}{\partial x} - \frac{\partial E_x}{\partial y} \right) \end{array} \right. \quad (1)$$

where E_x , E_y , E_z and H_x , H_y , H_z denote the components of the electric and magnetic fields respectively. The permittivity ε and permeability μ will in

general depend on the spatial location within the medium. If these electric and magnetic fields (multiplied by ε and μ respectively) start out divergence free, they will remain so when advanced forward in time by (1):

$$\begin{aligned} \frac{\partial}{\partial t} (\operatorname{div}(\varepsilon E)) &= \frac{\partial}{\partial t} \left(\frac{\partial(\varepsilon E_x)}{\partial x} + \frac{\partial(\varepsilon E_y)}{\partial y} + \frac{\partial(\varepsilon E_z)}{\partial z} \right) \\ &= \frac{\partial}{\partial x} \left(\frac{\partial H_z}{\partial y} - \frac{\partial H_y}{\partial z} \right) + \frac{\partial}{\partial y} \left(\frac{\partial H_x}{\partial z} - \frac{\partial H_z}{\partial x} \right) + \frac{\partial}{\partial z} \left(\frac{\partial H_y}{\partial x} - \frac{\partial H_x}{\partial y} \right) \\ &= 0 \end{aligned} \quad (2)$$

and similarly for $\operatorname{div}(\mu H)$. This implies that the relations $\operatorname{div}(\varepsilon E) = \rho$ (where ρ is the local charge density) and $\operatorname{div}(\mu H) = 0$ need not to be imposed as additional constraints. Neither of these quantities will change during wave propagation according to (1).

Arguably, the simplest possible finite difference approximation to (1) is obtained by approximating each derivative (whether in space or time) by centered second order accurate finite differences, i.e.

$$\begin{aligned} \frac{E_x|_{i,j,k}^{n+1} - E_x|_{i,j,k}^{n-1}}{2\Delta t} &= \frac{1}{\varepsilon} \left(\frac{H_z|_{i,j+1,k}^n - H_z|_{i,j-1,k}^n}{2\Delta y} - \frac{H_y|_{i,j,k+1}^n - H_y|_{i,j,k-1}^n}{2\Delta z} \right) \\ \frac{E_y|_{i,j,k}^{n+1} - E_y|_{i,j,k}^{n-1}}{2\Delta t} &= \frac{1}{\varepsilon} \left(\frac{H_x|_{i,j,k+1}^n - H_x|_{i,j,k-1}^n}{2\Delta z} - \frac{H_z|_{i+1,j,k}^n - H_z|_{i-1,j,k}^n}{2\Delta x} \right) \\ \frac{E_z|_{i,j,k}^{n+1} - E_z|_{i,j,k}^{n-1}}{2\Delta t} &= \frac{1}{\varepsilon} \left(\frac{H_y|_{i+1,j,k}^n - H_y|_{i-1,j,k}^n}{2\Delta x} - \frac{H_x|_{i,j+1,k}^n - H_x|_{i,j-1,k}^n}{2\Delta y} \right) \\ \frac{H_x|_{i,j,k}^{n+1} - H_x|_{i,j,k}^{n-1}}{2\Delta t} &= \frac{-1}{\mu} \left(\frac{E_z|_{i,j+1,k}^n - E_z|_{i,j-1,k}^n}{2\Delta y} - \frac{E_y|_{i,j,k+1}^n - E_y|_{i,j,k-1}^n}{2\Delta z} \right) \\ \frac{H_y|_{i,j,k}^{n+1} - H_y|_{i,j,k}^{n-1}}{2\Delta t} &= \frac{-1}{\mu} \left(\frac{E_x|_{i,j,k+1}^n - E_x|_{i,j,k-1}^n}{2\Delta z} - \frac{E_z|_{i+1,j,k}^n - E_z|_{i-1,j,k}^n}{2\Delta x} \right) \\ \frac{H_z|_{i,j,k}^{n+1} - H_z|_{i,j,k}^{n-1}}{2\Delta t} &= \frac{-1}{\mu} \left(\frac{E_y|_{i+1,j,k}^n - E_y|_{i-1,j,k}^n}{2\Delta x} - \frac{E_x|_{i,j+1,k}^n - E_x|_{i,j-1,k}^n}{2\Delta y} \right) \end{aligned} \quad (3)$$

In the style of (2), we can see that (3) at each grid point exactly preserves the value of discrete analogs of $\operatorname{div}(\varepsilon E)$ and $\operatorname{div}(\mu H)$.

2.1 Space Staggering

A key to the long-standing popularity of the Yee scheme (3) [44] is the concept of grid staggering. We illustrate this first in a simpler case, viz. for the scalar one-way wave equation $u_t + u_x = 0$. Centered approximations in space and time, on a Cartesian grid, result in two entirely separate interlaced computations over the grid points marked “x” and over those marked “o” in Fig. 1. By computing over only one of the sets, say, the point set marked “o”, we save a factor of two in computational effort. This also avoids trouble with

high-frequency oscillations, which would otherwise be the apparent manifestation of the two independent solutions over time most likely having drifted somewhat apart.

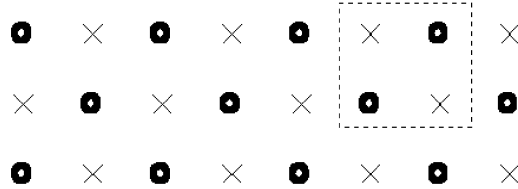


Fig. 1. Illustration of grid staggering in the x, t -plane for the one-way wave equation $u_t + u_x = 0$

The same concept of staggering applies also to Maxwell's equations in 3D, but gives then far larger savings – a factor of 16 rather than of two. Just like the grid in Fig. 1 is made up of lots of translates of a 'basic grid unit' (as displayed within the dotted frame), the 3D spatial lattice for the Yee scheme is made up of translates of the block shown in Fig. 2, stacked in 3D as indicated by Fig. 3. These figures show the spatial layout only (due to the difficulty of simultaneously displaying graphically time and three spatial dimensions). On alternate time levels, only the three E -components or only the three H -components are present, respectively, in the positions as shown in Fig. 2. Considering how data is coupled by (3), this very sparse data layout suffices for a complete calculation. Each variable appears only at one of eight corner nodes, and furthermore only at every second time level. Having all variables present at all nodes at all times would amount to carrying out 16 separate independent Yee calculations.

If there were no concerns about irregular geometries, it would be an easy matter to greatly improve the computational efficiency of the Yee scheme by just increasing the order of accuracy in both time and space (while maintaining the staggering of the variables). With a fixed grid spacing, standard finite difference approximations for the first derivative (in general for odd derivatives) are much more accurate half-way between grid points than at grid points [14] (with the advantage increasing with the order of the approximation). In space, we can therefore employ highly accurate finite difference (FD) approximations of increasing orders/stencil widths. Extensions to implicit staggered approximations are derived and analyzed in Fornberg and Ghrist [16]. The limits of increasing accuracy (stencil width) will in all cases correspond to the pseudospectral (PS) method (see also [11]).

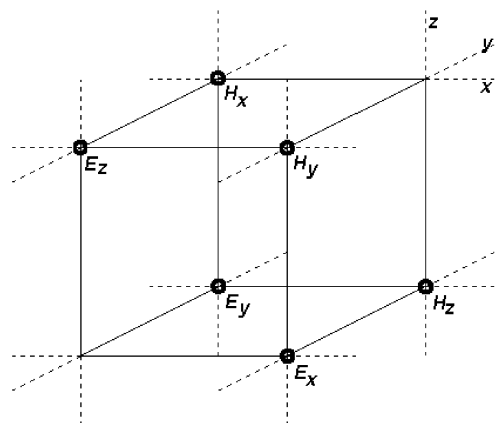


Fig. 2. Basic computational cell in the Yee scheme for Maxwell's equations. The E 's and H 's appear only at alternate time levels

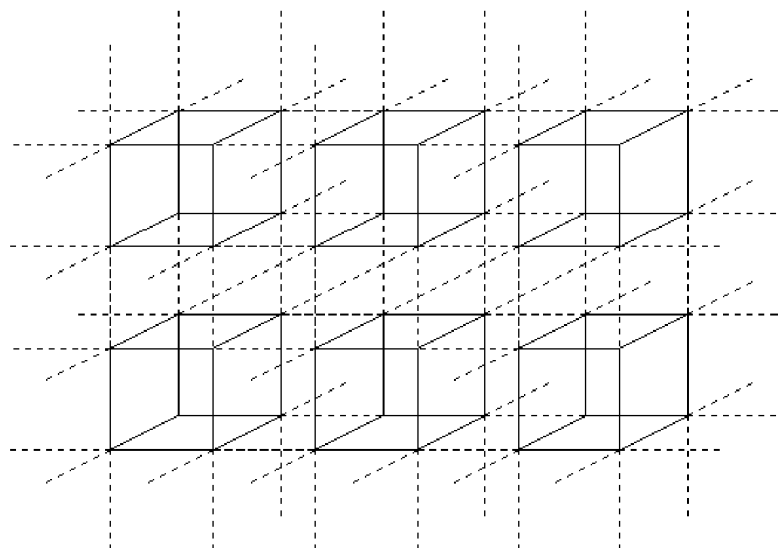


Fig. 3. Stacking of Yee cells of the form shown in the previous figure, in order to form a complete 3D Cartesian grid

2.2 Time Staggering

The stencils for a few standard classes of linear multistep schemes are shown in the left part of Fig. 4. Applied to an ODE (or system of ODEs) $y' = f(t, y)$,

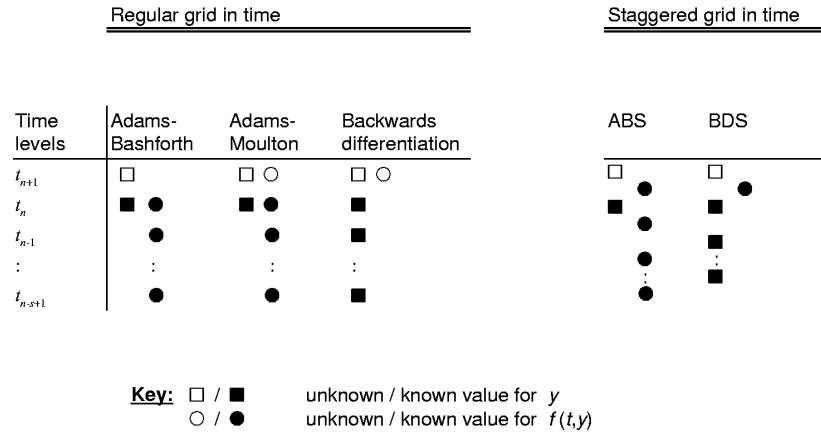


Fig. 4. Structure of some linear multistep methods for $y' = f(t, y)$

these require values of $f(t, y)$ to be available at the same time levels as are the y -values. Ghrist et al. [22] introduced recently a new class of time staggered ODE solvers. The staggered generalizations of Adams–Bashforth (AB), Adams–Moulton (AM) and backward differentiation (BD) become the explicit ABS and BDS schemes shown to the right. In the case of second order, these agree with the standard leap-frog scheme, but generalize this for higher orders of accuracy. To be applicable for wave equations (after method-of-lines discretization), the stability domains of the ODE solvers need to cover a section of the imaginary axis. Both for the regular AB and staggered ABS methods this occurs with orders 3,4, 7,8, 11,12, etc. Bounds on the imaginary axis coverage (which translates directly into CFL stability restrictions) and the leading truncation error constants are close to a factor of ten more favorable for the staggered than for the non-staggered methods. Since the ABS methods require no more operations or storage than the AB methods, they are generally much preferable. A possible exception can occur in cases of wave equations with damping. Like for the leap-frog scheme, all staggered ODE solvers lack negative real axis coverage in the stability domain. As a rule, if leap-frog discretization can be applied, so can also these (more effective) higher order generalizations.

The weights in the stencils for both the space approximations and the time stepping methods (implicit or explicit, staggered or not) are most conveniently obtained from the two-line symbolic algebra algorithm described in [12].

The lack of geometrical constraints in the time direction makes it particularly easy to use high order (big stencil) methods in that direction. The

main reason this is not routinely utilized has to do with stability. For the Yee scheme, it can be shown (for example by von Neumann analysis) that computations will be unstable unless $\Delta t < 1 / (c \sqrt{1/(\Delta x)^2 + 1/(\Delta y)^2 + 1/(\Delta z)^2})$, where $c = 1/\sqrt{\varepsilon\mu}$ is the wave speed. In this case, the actual stability constraint agrees exactly with the (often not sharp) upper bound on the time step imposed by the CFL (Courant–Friedrichs–Levy) condition. This condition usually makes it pointless to try to use higher order accuracy in time than what is used in space. Although doing so would increase the temporal accuracy, stability constraints would prevent this from being utilized to gain computational efficiency through the use of significantly larger time steps.

3 Situations Where Geometrical Features are Similar in Size to, or Larger Than a Typical Wave Length

As mentioned above, the choice of spatial discretization method is usually dictated by the complexity of material interfaces. In this first scenario – with geometrical features similar to or larger than a typical wave length – the main problem is one of approximating Maxwell's equations at curved boundaries accurately and economically. Boundary integral-type methods (see for example [1] and [39]) offer a potentially very powerful approach. Focusing here on discretizations of Maxwell's equations in the form (1), we will next make some very brief comments on four different implementation ideas.

3.1 Yee Scheme

We have already briefly described this scheme; much more detail can be found e.g. in Taflove and Hagness [42] or Kunz and Luebbers [28]. It can probably be said, without exaggeration, that this has been the main tool for FDTD (finite difference time domain) calculations over the last 30 years. Only recently has it started to give way to higher order methods and, in particular, to methods that adapt more flexibly to irregular geometries (rather than just relying on 'staircasing' – the approximation of all domains simply as subsets of the regularly stacked Yee cells). However, thanks to its ease-of-use in cases when accuracy and computational efficiency are not critical, it will probably remain of importance for the foreseeable future.

3.2 Finite Elements

Like for the Yee scheme, many books, as well as commercial program packages, have been entirely devoted to finite element (FE) methods for CEM. We will here make no attempt to survey this discipline, but refer the readers to [26] and [27]. In general, FE methods for CEM are particularly well suited for use in software packages, where high computational efficiency has been

traded for user-friendliness and convenience in applying different geometries, boundary conditions, etc. FEMLAB and ANSYS are two examples of widely available FE packages which specialize in structural mechanics, but for which very capable toolboxes for CEM are available. FE methods which can dynamically alter both gridding and element orders (*hp*-adaptive methods) can be very effective, but are very complicated to implement [5].

3.3 Finite Element–Finite Difference Hybrid Methods

Hybrid methods use different numerical methods in different regions of the computational domain. In one notable such development, Edelvik and Ledfelt [8] combine a geometrically flexible and unconditionally stable finite element discretization near boundaries with the much simpler and more cost-effective Yee scheme throughout the bulk of the domain. In a layer near the boundaries, the two grids share edges, as is indicated in the 2D illustration in Fig. 5. The FE part gives rise to a positive definite system that is effectively solved, at each time step, by pre-conditioned conjugate gradients (typically converging in around 10–20 iterations). For the region of overlap, a procedure is used that combines the results from the two domains in a way that ensures both accuracy and overall stability [38]. Fig. 6 illustrates a very small section of the 3D grid used in a simulation of electromagnetic fields that would arise inside the cockpit area of a SAAB 2000 aircraft, if the plane was struck by lightning. In the cockpit area, a tetrahedral-type FE grid is used for both the outside skin and for interior structures. Shortly outside the skin, we see a transition to a box-like Yee grid which continues (not shown) to fill a volume surrounding the plane. Since, in this particular application, the interest is confined to the cockpit area, objects further back (like wings, engines, etc. outside the section displayed in Fig. 6) were all staircased. Computations with around 10^6 cells and 7000 time steps take around 2 days on a typical single processor workstation.

Many variations are possible. For example El Hachemi [9] uses interpolation between the FD and FE areas (as an alternative option to letting the grids share edges).

3.4 Spectral Elements

Several variations of spectral element-type methods have been proposed, in particular for computational fluid dynamics, but also for Maxwell’s equations. The method by Hesthaven and Warburton [25] is notable in several ways: arbitrary order of accuracy, stability and convergence are strictly proven, and an element coupling is used which permits very effective distributed memory parallel implementation. Furthermore, very large-scale computations have been successfully demonstrated in 3D (in particular for radar scattering from aircraft). In 3D, the volume of interest is divided up into tetrahedra

(some of which can be curvilinear for best fit with objects). Within each such element, the unknowns are represented by a single polynomial in the three space variables. If the degree is chosen as n , this polynomial will have $\frac{1}{6}(n+1)(n+2)(n+3)$ coefficients. That is then also the number of node points for such a tetrahedron. Their positions have been optimized to provide a particularly good interpolation capability, resulting in a certain distribution with $\frac{1}{2}(n+1)(n+2)$ node points on each face (including one at each tetrahedral corner and some along each edge), and the rest inside. While some spectral element methods couple different elements in ways to achieve a high degree of overall smoothness, the approach taken here is one of discontinuous Galerkin form, and with boundary conditions enforced only weakly through a penalty term. Data exchanges between the elements are based on characteristic information at their outer surfaces (a key to effective parallelism based on domain decomposition). Although a hybrid approach (involving a simpler gridding and numerical scheme away from interfaces) has not yet been implemented with this method, the developers are considering such a change (for which conditional stability will remain assured). For more specific information on the method, see [25].

A large part of the modeling effort in FDTD is often associated with grid generation. One of the strengths of this spectral element approach (like for hp -adaptive FE methods) is that it can utilize even a coarse and skewed grid, and then reach a required accuracy by means of increasing the order within each element (rather than requiring a new and better gridding; typically a more expensive proposition). Fig. 7 is a 2D illustration of this. The starting point is a deliberately skewed and coarse grid, as shown in the top left subplot

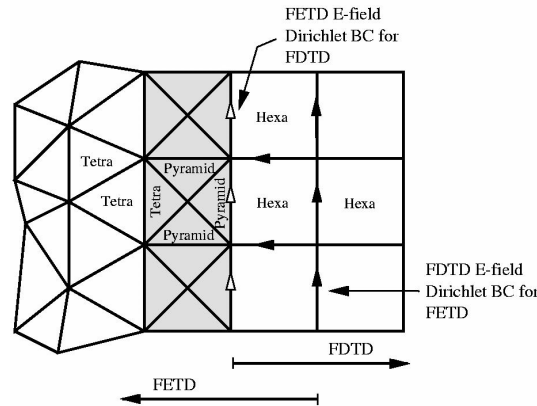


Fig. 5. Schematic illustration of transition between FE and FD areas of the FE-FD hybrid method

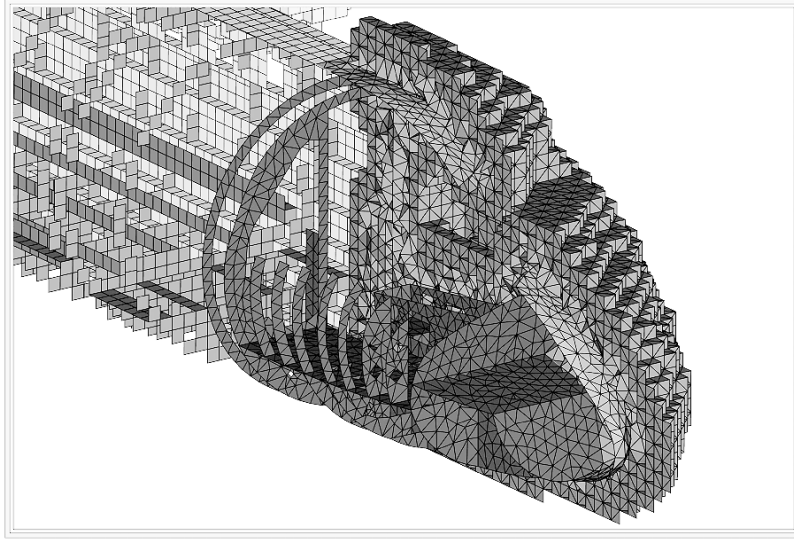


Fig. 6. Example of FE-FD gridding of the cockpit area of a Saab 2000 aircraft

(with the internal mesh in each triangle, corresponding to order $n = 10$, also displayed). The additional three subplots show how bringing up the order within the spectral elements produces convergence to the vertically symmetric scattered field that results when plane waves arrive from the left.

3.5 Block-Pseudospectral Method

Of the approaches we are commenting on here, this one is the least well tested. It was introduced by Driscoll and Fornberg [7], and was shown to be highly effective in quite simple 2D geometries, such as the one shown in Fig. 8. The basic idea is somewhat similar to the FE-FD hybrid approach described above, but pushed a lot further towards high orders of accuracy in exchange for reduced geometric flexibility and a less clear stability situation. In the main part of the domain – away from objects – all spatial derivatives are approximated on an equi-spaced Cartesian grid by the implicit and staggered formula

$$\frac{9}{80} u'(x-h) + \frac{31}{40} u'(x) + \frac{9}{80} u'(x+h) = \frac{1}{h} \left[-\frac{17}{240} u(x-\frac{3}{2}h) - \frac{63}{80} u(x-\frac{1}{2}h) + \frac{63}{80} u(x+\frac{1}{2}h) + \frac{17}{240} u(x+\frac{3}{2}h) \right] + O(h^6).$$

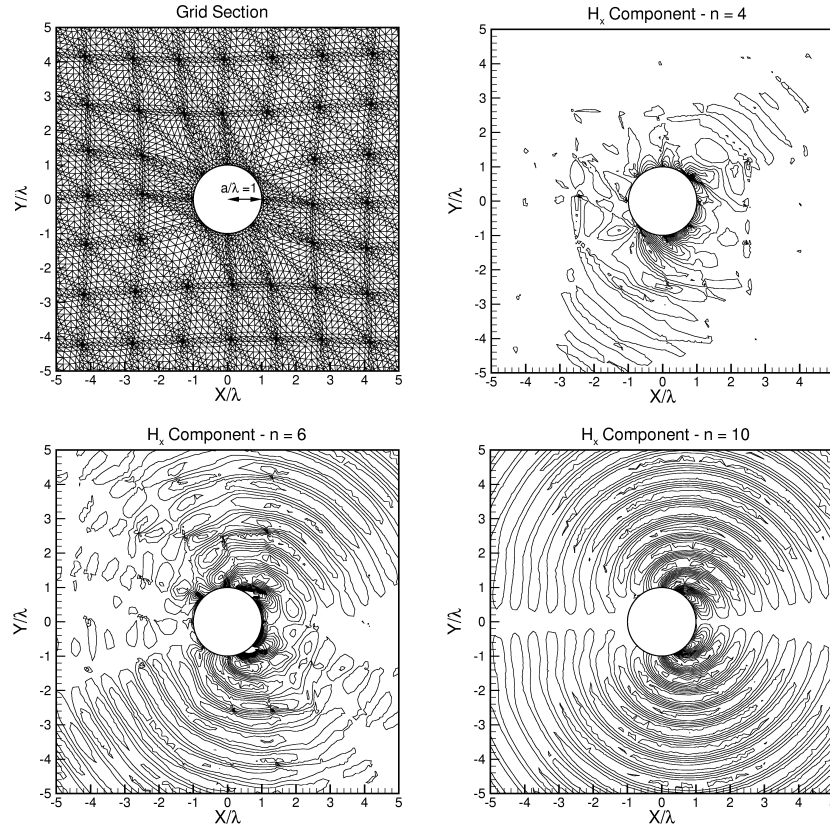


Fig. 7. Intentionally skewed gridding around a cylinder (with internal nodes for $n = 10$ shown; top left), and the scattered fields for $n = 4, 6,$ and 10

This approximation (one example of a wide class of similar formulas derived and analyzed in [16]) features a particularly small constant within the $O(h^6)$ error term, is quite compact, and leads only to tridiagonal systems to solve. In the circular strips that fit the outer shape of the conductors, Chebyshev-like pseudospectral discretization was used across the strips (implemented via a differentiation matrix and not via FFTs, since there are only 6 grid points in total in that direction), and the Fourier pseudospectral method was used around the strips. (For an overview of pseudospectral methods, see [11].) Data were interpolated between the grids in the regions of overlap, and the standard fourth order Runge–Kutta scheme was used for the time integration. The simulation shown in Fig. 9 was achieved by putting together these quite standard numerical ingredients. The grid densities in the different regions were precisely as shown by dots and lines in Fig. 8. The resolution in this

example was approximately 3–4 PPW, which can be compared to around the 50–60 PPW that would have been required to reach a similar accuracy with a Yee scheme. With so many fewer points needed for the higher order method *in each space dimension* (together with a low computational cost per grid point), the savings in both memory and computer time become very large.

In another test, the objects were inclined flat plates (rather than cylinders). The boundary fitting grids then used Chebyshev-type node distributions in both directions within rectangular patches. By including large numbers of such patches – which themselves can overlap – it is anticipated (but as yet not tested) that generalizations to more complex regions and to 3D will become possible. Although the 2D test cases were found to be stable, entirely without the inclusion of any artificial damping, stability has not been strictly proven. This could possibly become a significant issue in more complex settings.

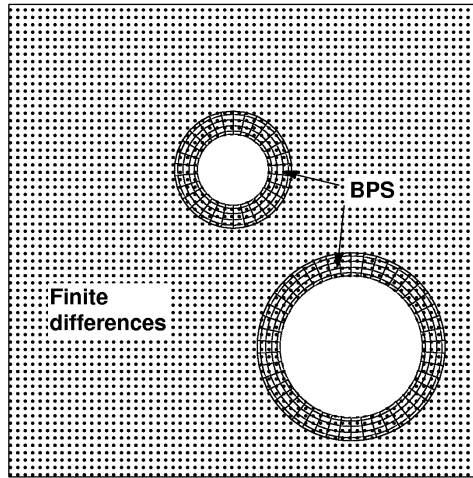


Fig. 8. Grids, with actual discretization sizes shown (by dots and by lines) for the test case of a wave front impinging on two perfect conductors

Concluding this brief discussion of some numerical approaches, we would like to re-emphasize that efficient computation in free space and in the immediate vicinity of interfaces pose very different numerical challenges. Quite different numerical methods are usually preferable, suggesting that hybrid methods are a natural approach to pursue.

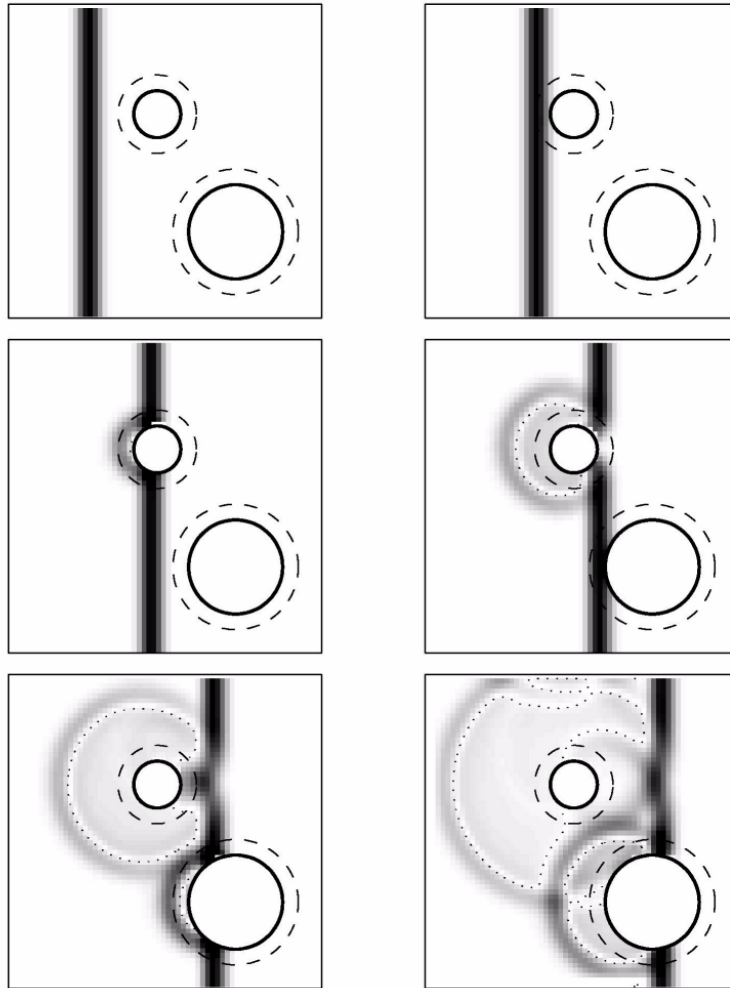


Fig. 9. Simulation of an electromagnetic wave front being scattered from two perfectly conducting cylinders

4 Situations Where Geometrical Features are Much Smaller Than a Typical Wave Length

In the cases mentioned in the Introduction (integrated circuits, cellular phones, and lightning strikes), the spatial scales are about 10^{-5} wave lengths in size. The spatial gridding then needs to be correspondingly fine in order

to capture the geometry properly, i.e. we are forced to an extreme over-sampling in space compared to what would have been needed if the goal was only to resolve a wave. Such very detailed grids, especially in 3D, will contain vast numbers of grid points (even if used only in small areas of the overall computational domain). To keep computational costs manageable, the time stepping procedure needs to be explicit (or nearly so). The CFL stability condition then tells that the time step also will need to be extremely small. The dilemma in this situation is that, while the accuracy in time can be met by using a time step that is some moderate fraction of the wave length, stability would seem to impose upper time steps bounds of maybe only 10^{-5} of this size. In order not to incur the vast expense of using such minute time steps, some approach needs to be found which essentially bypasses the restriction that is usually imposed by the CFL condition. In cases when the grids are refined only in very small areas, it can be very convenient to still be able to use the same (long) time steps everywhere.

Two discretization methods have very recently been proposed which feature unconditional stability. Although this property has been strictly proven mainly for periodic problems in the case of a constant medium, the practical experience is very favorable also for variable medium initial-boundary value problems, as well as in combination with PML (perfectly matched layer) far-field boundary conditions. Compared to the Yee scheme, each of the new methods costs about four times as much as per time step – a small price to pay for being able to use a time step many orders of magnitude larger than would otherwise be possible. We will describe these two methods in the remainder of this section.

4.1 Alternating Direction Implicit (ADI) Method

The ADI approach has been very successful for parabolic and elliptic PDEs for the last 50 years. Seminal papers in the area include e.g. [6] and [35]. Similar 3-stage dimensional splittings for the 3D Maxwell's equations have been repeatedly tried in various forms since then, but have invariably fallen short of the goal of unconditional time stability. However, a 2-stage splitting introduced in 1999 by Zheng et al. [46, 47] does achieve this goal. The original way to state this scheme includes introducing a half-way time level $n + 1/2$ between the adjacent time levels n and $n + 1$. We advance our six variables as follows.

Stage 1:

$$\begin{aligned}
 \frac{E_x|_{i,j,k}^{n+1/2} - E_x|_{i,j,k}^n}{\Delta t/2} &= \frac{1}{\varepsilon} \left(\frac{H_z|_{i,j+1,k}^{n+1/2} - H_z|_{i,j-1,k}^{n+1/2}}{2\Delta y} - \frac{H_y|_{i,j,k+1}^n - H_y|_{i,j,k-1}^n}{2\Delta z} \right) \\
 \frac{E_y|_{i,j,k}^{n+1/2} - E_y|_{i,j,k}^n}{\Delta t/2} &= \frac{1}{\varepsilon} \left(\frac{H_x|_{i,j,k+1}^{n+1/2} - H_x|_{i,j,k-1}^{n+1/2}}{2\Delta z} - \frac{H_z|_{i+1,j,k}^n - H_z|_{i-1,j,k}^n}{2\Delta x} \right) \\
 \frac{E_z|_{i,j,k}^{n+1/2} - E_z|_{i,j,k}^n}{\Delta t/2} &= \frac{1}{\varepsilon} \left(\frac{H_y|_{i+1,j,k}^{n+1/2} - H_y|_{i-1,j,k}^{n+1/2}}{2\Delta x} - \frac{H_x|_{i,j+1,k}^n - H_x|_{i,j-1,k}^n}{2\Delta y} \right) \\
 \frac{H_x|_{i,j,k}^{n+1/2} - H_x|_{i,j,k}^n}{\Delta t/2} &= \frac{1}{\mu} \left(\frac{E_y|_{i,j,k+1}^{n+1/2} - E_y|_{i,j,k-1}^{n+1/2}}{2\Delta z} - \frac{E_z|_{i,j+1,k}^n - E_z|_{i,j-1,k}^n}{2\Delta y} \right) \\
 \frac{H_y|_{i,j,k}^{n+1/2} - H_y|_{i,j,k}^n}{\Delta t/2} &= \frac{1}{\mu} \left(\frac{E_z|_{i+1,j,k}^{n+1/2} - E_z|_{i-1,j,k}^{n+1/2}}{2\Delta x} - \frac{E_x|_{i,j,k+1}^n - E_x|_{i,j,k-1}^n}{2\Delta z} \right) \\
 \frac{H_z|_{i,j,k}^{n+1/2} - H_z|_{i,j,k}^n}{\Delta t/2} &= \frac{1}{\mu} \left(\frac{E_x|_{i,j+1,k}^{n+1/2} - E_x|_{i,j-1,k}^{n+1/2}}{2\Delta y} - \frac{E_y|_{i+1,j,k}^n - E_y|_{i-1,j,k}^n}{2\Delta x} \right)
 \end{aligned} \tag{4}$$

Stage 2:

$$\begin{aligned}
 \frac{E_x|_{i,j,k}^{n+1} - E_x|_{i,j,k}^{n+1/2}}{\Delta t/2} &= \frac{1}{\varepsilon} \left(\frac{H_z|_{i,j+1,k}^{n+1/2} - H_z|_{i,j-1,k}^{n+1/2}}{2\Delta y} - \frac{H_y|_{i,j,k+1}^{n+1} - H_y|_{i,j,k-1}^{n+1}}{2\Delta z} \right) \\
 \frac{E_y|_{i,j,k}^{n+1} - E_y|_{i,j,k}^{n+1/2}}{\Delta t/2} &= \frac{1}{\varepsilon} \left(\frac{H_x|_{i,j,k+1}^{n+1/2} - H_x|_{i,j,k-1}^{n+1/2}}{2\Delta z} - \frac{H_z|_{i+1,j,k}^{n+1} - H_z|_{i-1,j,k}^{n+1}}{2\Delta x} \right) \\
 \frac{E_z|_{i,j,k}^{n+1} - E_z|_{i,j,k}^{n+1/2}}{\Delta t/2} &= \frac{1}{\varepsilon} \left(\frac{H_y|_{i+1,j,k}^{n+1/2} - H_y|_{i-1,j,k}^{n+1/2}}{2\Delta x} - \frac{H_x|_{i,j+1,k}^{n+1} - H_x|_{i,j-1,k}^{n+1}}{2\Delta y} \right) \\
 \frac{H_x|_{i,j,k}^{n+1} - H_x|_{i,j,k}^{n+1/2}}{\Delta t/2} &= \frac{1}{\mu} \left(\frac{E_y|_{i,j,k+1}^{n+1/2} - E_y|_{i,j,k-1}^{n+1/2}}{2\Delta z} - \frac{E_z|_{i,j+1,k}^{n+1} - E_z|_{i,j-1,k}^{n+1}}{2\Delta y} \right) \\
 \frac{H_y|_{i,j,k}^{n+1} - H_y|_{i,j,k}^{n+1/2}}{\Delta t/2} &= \frac{1}{\mu} \left(\frac{E_z|_{i+1,j,k}^{n+1/2} - E_z|_{i-1,j,k}^{n+1/2}}{2\Delta x} - \frac{E_x|_{i,j,k+1}^{n+1} - E_x|_{i,j,k-1}^{n+1}}{2\Delta z} \right) \\
 \frac{H_z|_{i,j,k}^{n+1} - H_z|_{i,j,k}^{n+1/2}}{\Delta t/2} &= \frac{1}{\mu} \left(\frac{E_x|_{i,j+1,k}^{n+1/2} - E_x|_{i,j-1,k}^{n+1/2}}{2\Delta y} - \frac{E_y|_{i+1,j,k}^{n+1} - E_y|_{i-1,j,k}^{n+1}}{2\Delta x} \right)
 \end{aligned} \tag{5}$$

Several things can be noted.

- The stages differ in that we swap which of the two terms in each right hand side (RHS) that is discretized on the new and on the old time level.
- On each new time level, we can obtain tridiagonal linear systems for E_x , E_y , E_z . For example in Stage 1, on the new time level, we can eliminate H_z between the first and the last equation, giving a tridiagonal system for E_x . Once we similarly get (and solve) the tridiagonal systems also for E_y and E_z , the remaining variables H_x , H_y , H_z follow explicitly.
- Yee-type staggering can again be applied, but only in space, giving savings of a factor of 8 (rather than 16) compared to the case when all variables are represented at all grid points.

- The solution at the intermediate time level $n + 1/2$ is only first order accurate. However, the accuracy is second order after each completed pair of stages (i.e. at all integer-numbered time levels).

Shortly after this ADI scheme was first proposed, Namiki [33] demonstrated its practical advantages for two test problems (a monopole antenna near a thin dielectric wall, and a stripline with a narrow gap). This scheme has also, by Liu and Gedney [31], been found to work well together with PML far field boundary conditions.

Proof of Unconditional Stability The original stability proof (in the case of a constant medium in a periodic or infinite domain) was first given in [47] and reproduced in [42]. It uses von Neumann analysis. This leads to the demanding task of analytically determining the eigenvalues of a certain 6×6 matrix, whose entries are functions of the grid steps and wave numbers. This does prove feasible, but only through some quite heavy use of computational symbolic algebra. It transpires that all the eigenvalues have magnitude one, which establishes the unconditional stability. The following simpler energy-based stability proof was given by Fornberg [13]. A third proof, based on the alternate ADI description in Sect. 4.1, is given in [4].

As we noted above, the ADI scheme is best laid out on a staggered Yee-type grid in space, but with no staggering in time. However, for the sake of simplifying the notation, we apply it here on a regular grid in space (i.e. a grid with every one of the six quantities E_x , E_y , E_z , H_x , H_y , H_z represented at each grid location, rather than at only one out of eight such locations). If we can prove unconditional stability in this regular grid case, we have of course also proven it for the 8 uncoupled sub-problems that it contains. Our energy method for showing that no Fourier mode can diverge as time increases starts by considering the ADI scheme over an arbitrary-sized periodic box. We then demonstrate that the sum of the squares of all the unknowns remain bounded for all times.

We again assume that ε and μ are constants, let $\alpha_x = \frac{\Delta t}{2\varepsilon\Delta x}$, $\beta_x = \frac{\Delta t}{2\mu\Delta x}$, and introduce similarly α_y , α_z , β_y and β_z . Separating the terms in (4) according to their time level gives

$$\begin{aligned}
E_x|_{i,j,k}^{n+1/2} - \alpha_y \left(H_z|_{i,j+1,k}^{n+1/2} - H_z|_{i,j-1,k}^{n+1/2} \right) &= E_x|_{i,j,k}^n - \alpha_z \left(H_y|_{i,j,k+1}^n - H_y|_{i,j,k-1}^n \right) \\
E_y|_{i,j,k}^{n+1/2} - \alpha_z \left(H_x|_{i,j,k+1}^{n+1/2} - H_x|_{i,j,k-1}^{n+1/2} \right) &= E_y|_{i,j,k}^n - \alpha_x \left(H_z|_{i+1,j,k}^n - H_z|_{i-1,j,k}^n \right) \\
E_z|_{i,j,k}^{n+1/2} - \alpha_x \left(H_y|_{i+1,j,k}^{n+1/2} - H_y|_{i-1,j,k}^{n+1/2} \right) &= E_z|_{i,j,k}^n - \alpha_y \left(H_x|_{i,j+1,k}^n - H_x|_{i,j-1,k}^n \right) \\
H_x|_{i,j,k}^{n+1/2} - \beta_z \left(E_y|_{i,j,k+1}^{n+1/2} - E_y|_{i,j,k-1}^{n+1/2} \right) &= H_x|_{i,j,k}^n - \beta_y \left(E_z|_{i,j+1,k}^n - E_z|_{i,j-1,k}^n \right) \\
H_y|_{i,j,k}^{n+1/2} - \beta_x \left(E_z|_{i+1,j,k}^{n+1/2} - E_z|_{i-1,j,k}^{n+1/2} \right) &= H_y|_{i,j,k}^n - \beta_z \left(E_x|_{i,j,k+1}^n - E_x|_{i,j,k-1}^n \right) \\
H_z|_{i,j,k}^{n+1/2} - \beta_y \left(E_x|_{i,j+1,k}^{n+1/2} - E_x|_{i,j-1,k}^{n+1/2} \right) &= H_z|_{i,j,k}^n - \beta_x \left(E_y|_{i+1,j,k}^n - E_y|_{i-1,j,k}^n \right)
\end{aligned} \tag{6}$$

We next take the square of both sides of each equation above; then multiply the first three equations by ε and the next three by μ . For example, in

the case of the first and the fifth equations of (6), this gives

$$\begin{aligned}
 & \varepsilon \alpha_y^2 \left(H_z|_{i,j+1,k}^{n+1/2} - H_z|_{i,j-1,k}^{n+1/2} \right)^2 - \frac{\Delta t}{\Delta y} E_x|_{i,j,k}^{n+1/2} \left(H_z|_{i,j+1,k}^{n+1/2} - H_z|_{i,j-1,k}^{n+1/2} \right) \\
 & \quad + \varepsilon \left(E_x|_{i,j,k}^{n+1/2} \right)^2 = \varepsilon \left(E_x|_{i,j,k}^n \right)^2 + \varepsilon \alpha_z^2 \left(H_y|_{i,j,k+1}^n - H_y|_{i,j,k-1}^n \right)^2 \\
 & \quad \quad \quad - \frac{\Delta t}{\Delta z} E_x|_{i,j,k}^n \left(H_y|_{i,j,k+1}^n - H_y|_{i,j,k-1}^n \right) \\
 \\
 & \mu \beta_x^2 \left(E_z|_{i+1,j,k}^{n+1/2} - E_z|_{i-1,j,k}^{n+1/2} \right)^2 - \frac{\Delta t}{\Delta x} H_y|_{i,j,k}^{n+1/2} \left(E_z|_{i+1,j,k}^{n+1/2} - E_z|_{i-1,j,k}^{n+1/2} \right) \\
 & \quad + \mu \left(H_y|_{i,j,k}^{n+1/2} \right)^2 = \mu \left(H_y|_{i,j,k}^n \right)^2 + \mu \beta_z^2 \left(E_x|_{i,j,k+1}^n - E_x|_{i,j,k-1}^n \right)^2 \\
 & \quad \quad \quad - \frac{\Delta t}{\Delta z} H_y|_{i,j,k}^n \left(E_x|_{i,j,k+1}^n - E_x|_{i,j,k-1}^n \right)
 \end{aligned}$$

If we add these two equations together, one of the expressions on the right hand side will become

$$-\frac{\Delta t}{\Delta z} \left\{ E_x|_{i,j,k}^n \left(H_y|_{i,j,k+1}^n - H_y|_{i,j,k-1}^n \right) + H_y|_{i,j,k}^n \left(E_x|_{i,j,k+1}^n - E_x|_{i,j,k-1}^n \right) \right\}.$$

When summing this expression over the full 3D periodic volume, it cancels out to become zero (as can be seen directly, or by summation by parts; already summing in the z -direction makes it zero, and further summation in the x - and y -directions of zeros remain zero). In the same way, when we add the squares of *all* the relations in (6) over the full volume, all the products that mix E and H -terms will cancel out on both of the time levels $n + 1/2$ and n . Hence, we get $\sum_{(1)}^{n+1/2} = \sum_{(2)}^n$, where

$$\begin{aligned}
 \sum_{(1)}^{n+1/2} = \sum_{i,j,k} \left\{ \varepsilon \left[\left(E_x|_{i,j,k}^{n+1/2} \right)^2 + \left(E_y|_{i,j,k}^{n+1/2} \right)^2 + \left(E_z|_{i,j,k}^{n+1/2} \right)^2 \right] \right. \\
 \quad \quad \quad \left. + \mu \left[\left(H_x|_{i,j,k}^{n+1/2} \right)^2 + \left(H_y|_{i,j,k}^{n+1/2} \right)^2 + \left(H_z|_{i,j,k}^{n+1/2} \right)^2 \right] \right. \\
 \quad + \varepsilon \left[\alpha_y^2 \left(H_x|_{i,j,k+1}^{n+1/2} - H_x|_{i,j,k-1}^{n+1/2} \right)^2 + \alpha_z^2 \left(H_y|_{i+1,j,k}^{n+1/2} - H_y|_{i-1,j,k}^{n+1/2} \right)^2 \right. \\
 \quad + \alpha_x^2 \left(H_z|_{i,j+1,k}^{n+1/2} - H_z|_{i,j-1,k}^{n+1/2} \right)^2 \left. \right] + \mu \left[\beta_z^2 \left(E_x|_{i,j+1,k}^{n+1/2} - E_x|_{i,j-1,k}^{n+1/2} \right)^2 \right. \\
 \quad \quad \quad \left. \left. + \beta_x^2 \left(E_y|_{i,j,k+1}^{n+1/2} - E_y|_{i,j,k-1}^{n+1/2} \right)^2 + \beta_y^2 \left(E_z|_{i+1,j,k}^{n+1/2} - E_z|_{i-1,j,k}^{n+1/2} \right)^2 \right] \right\}
 \end{aligned}$$

and

$$\begin{aligned}
\sum_{(2)}^n &= \sum_{i,j,k} \left\{ \varepsilon \left[(E_x|_{i,j,k}^n)^2 + (E_y|_{i,j,k}^n)^2 + (E_z|_{i,j,k}^n)^2 \right] \right. \\
&\quad \left. + \mu \left[(H_x|_{i,j,k}^n)^2 + (H_y|_{i,j,k}^n)^2 + (H_z|_{i,j,k}^n)^2 \right] \right. \\
&\quad + \varepsilon \left[\alpha_z^2 (H_x|_{i,j+1,k}^n - H_x|_{i,j-1,k}^n)^2 + \alpha_x^2 (H_y|_{i,j,k+1}^n - H_y|_{i,j,k-1}^n)^2 \right. \\
&\quad \left. + \alpha_y^2 (H_z|_{i+1,j,k}^n - H_z|_{i-1,j,k}^n)^2 \right] + \mu \left[\beta_y^2 (E_x|_{i,j,k+1}^n - E_x|_{i,j,k-1}^n)^2 \right. \\
&\quad \left. + \beta_z^2 (E_y|_{i+1,j,k}^n - E_y|_{i-1,j,k}^n)^2 + \beta_x^2 (E_z|_{i,j+1,k}^n - E_z|_{i,j-1,k}^n)^2 \right] \left. \right\}.
\end{aligned}$$

The superscript on each of the each of the sums $\sum_{(1)}^{n+1/2}$ and $\sum_{(2)}^n$ denotes the time level, and the subscript indicates that the two sums furthermore differ a bit subtly in the indices and coefficients for the terms that contain differences.

Exactly in the same way as we have arrived at $\sum_{(1)}^{n+1/2} = \sum_{(2)}^n$ starting from the Stage 1 equations (4), we could instead have started from the Stage 2 equations (5) to obtain $\sum_{(2)}^{n+1} = \sum_{(1)}^{n+1/2}$. This tells that $\sum_{(2)}^{n+1} = \sum_{(2)}^n$, i.e. after each completed full time step, $\sum_{(2)}$ remains unchanged. The expression

$$\begin{aligned}
\sum^n &= \sum_{i,j,k} \left\{ \varepsilon \left[(E_x|_{i,j,k}^n)^2 + (E_y|_{i,j,k}^n)^2 + (E_z|_{i,j,k}^n)^2 \right] \right. \\
&\quad \left. + \mu \left[(H_x|_{i,j,k}^n)^2 + (H_y|_{i,j,k}^n)^2 + (H_z|_{i,j,k}^n)^2 \right] \right\}
\end{aligned}$$

appears in $\sum_{(2)}^n$ together with additional terms that are all squares of differences, and therefore are guaranteed to be positive. Since $\sum_{(2)}^n$ is preserved for all times (all integer values of n), the sum \sum^n will be uniformly bounded for all times by the initial value of $\sum_{(2)}^n$. This implies that the ADI method is unconditionally stable.

A major advantage with ‘energy-type’ proofs, like the present, is that they can often be extended to hold also in the case of variable coefficients (i.e. variable media) and for different types of boundary conditions. This has already been carried out for a box-shaped cavity with perfectly conducting walls by Gao et al. [20].

Alternative Description of the ADI Method The 3D Maxwell’s equations (1) can be written

$$\frac{\partial}{\partial t} \begin{bmatrix} E_x \\ E_y \\ E_z \\ H_x \\ H_y \\ H_z \end{bmatrix} = \begin{bmatrix} \frac{1}{\varepsilon} \frac{\partial H_z}{\partial y} \\ \frac{1}{\varepsilon} \frac{\partial H_x}{\partial z} \\ \frac{1}{\varepsilon} \frac{\partial H_y}{\partial x} \\ \frac{1}{\varepsilon} \frac{\partial E_y}{\partial x} \\ \frac{\mu}{\varepsilon} \frac{\partial E_z}{\partial z} \\ \frac{\mu}{\varepsilon} \frac{\partial E_x}{\partial x} \\ \frac{1}{\mu} \frac{\partial E_x}{\partial y} \end{bmatrix} + \begin{bmatrix} -\frac{1}{\varepsilon} \frac{\partial H_y}{\partial z} \\ -\frac{1}{\varepsilon} \frac{\partial H_z}{\partial x} \\ -\frac{1}{\varepsilon} \frac{\partial H_x}{\partial y} \\ -\frac{1}{\varepsilon} \frac{\partial E_z}{\partial z} \\ -\frac{\mu}{\varepsilon} \frac{\partial E_y}{\partial y} \\ -\frac{1}{\mu} \frac{\partial E_y}{\partial x} \\ -\frac{1}{\mu} \frac{\partial E_x}{\partial z} \end{bmatrix} \quad (7)$$

or, more briefly,

$$\frac{\partial \underline{u}}{\partial t} = A \underline{u} + B \underline{u}.$$

The standard Crank–Nicolson discretisation in time is

$$\begin{aligned} \frac{\underline{u}^{n+1} - \underline{u}^n}{\Delta t} &= \frac{1}{2}(A\underline{u}^{n+1} + A\underline{u}^n) + \frac{1}{2}(B\underline{u}^{n+1} + B\underline{u}^n) + O(\Delta t)^2 \\ \Rightarrow \left(1 - \frac{\Delta t}{2}A - \frac{\Delta t}{2}B\right) \underline{u}^{n+1} &= \left(1 + \frac{\Delta t}{2}A + \frac{\Delta t}{2}B\right) \underline{u}^n + O(\Delta t)^3 \\ \Rightarrow \underbrace{\left(1 - \frac{\Delta t}{2}A\right) \left(1 - \frac{\Delta t}{2}B\right) \underline{u}^{n+1}}_{\text{One-step approximation}} &= \underbrace{\left(1 + \frac{\Delta t}{2}A\right) \left(1 + \frac{\Delta t}{2}B\right) \underline{u}^n}_{\text{One-step approximation}} \\ &+ \underbrace{\frac{(\Delta t)^2}{4} AB(\underline{u}^{n+1} - \underline{u}^n)}_{\text{Error} = O(\Delta t)^3} + O(\Delta t)^3. \end{aligned} \quad (8)$$

The ‘one-step approximation’

$$\left(1 - \frac{\Delta t}{2}A\right) \left(1 - \frac{\Delta t}{2}B\right) \underline{u}^{n+1} = \left(1 + \frac{\Delta t}{2}A\right) \left(1 + \frac{\Delta t}{2}B\right) \underline{u}^n \quad (9)$$

can be written in two stages

$$\begin{cases} \left(1 - \frac{\Delta t}{2}A\right) \underline{u}^{n+1/2} = \left(1 + \frac{\Delta t}{2}B\right) \underline{u}^n \\ \left(1 - \frac{\Delta t}{2}B\right) \underline{u}^{n+1} = \left(1 + \frac{\Delta t}{2}A\right) \underline{u}^{n+1/2}. \end{cases} \quad (10)$$

To verify this, we multiply the first equation of (10) by $\left(1 + \frac{\Delta t}{2}A\right)$ and the second one by $\left(1 - \frac{\Delta t}{2}A\right)$. The LHS of the first equation then equals the RHS of the second equation, and (9) follows. It is straightforward to verify that the two equations in (10) – after space derivatives in A and B have been replaced by centered finite differences – become equivalent to the two stages (4) and (5) of the ADI scheme. This way of deriving the ADI method offers us several advantages.

- We recognize that $\underline{u}^{n+1/2}$ more naturally can be seen just as an intermediate computational quantity rather than as some specific intermediate time level (at which we have reduced accuracy).
- The second order accuracy in time for the overall procedure has become obvious.
- It becomes easy to determine the precise form of the local temporal error (which will be of importance to us later for implementing deferred correction in order to reach higher orders of accuracy in time).

4.2 Crank–Nicolson Based Split-Step Method (CNS)

We start this subsection by briefly reviewing the general concept and history of split step methods, and we then note how they can be applied to the Maxwell’s equations.

Concept In the simplest form of split step, featuring only first order accuracy in time, one would advance an ODE (or a system of ODEs)

$$u_t = A(u) + B(u) \tag{11}$$

from time t to time $t + \Delta t$ by successively solving

$$\begin{aligned} u_t &= 2A(u) && \text{from } t \text{ to } t + \frac{1}{2}\Delta t, \text{ followed by} \\ u_t &= 2B(u) && \text{from } t + \frac{1}{2}\Delta t \text{ to } t + \Delta t \end{aligned}$$

Here, $A(u)$ and $B(u)$ can be very general nonlinear operators (in particular, there is no requirement that A and B commute). The two time increments are each of length $\frac{1}{2}\Delta t$. We therefore denote this splitting by $\{\frac{1}{2}, \frac{1}{2}\}$. One obtains second order accuracy in time by instead alternating the two equations in the pattern A, B, A while using the time increments $\{\frac{1}{4}, \frac{1}{2}, \frac{1}{4}\}$ – known as ‘Strang splitting’ [40]. In 1990 Yoshida [45] devised a systematic way to obtain similar split step methods of still higher orders. From an implementation standpoint, one simply chooses certain longer time increment sequences, while again alternating A, B, A, B, \dots . Table 1 shows the coefficients of methods of orders 1, 2, 4, 6, and 8. The coefficients for the methods of order 6 and above are not unique.

The split step approach is especially interesting for PDEs. If such an equation is of the form $u_t + A(u, u_x) + B(u, u_y) = 0$, immediate dimensional splitting leads to two 1D problems. Splitting is also of significant interest for certain nonlinear wave equations (see e.g. [15] for comparisons between split step and two other approaches). For example, the Korteweg–de Vries (KdV) equation $u_t + uu_x + u_{xxx} = 0$ can be split into $u_t + 2uu_x = 0$ (which features few numerical difficulties over brief times) and $u_t + 2u_{xxx} = 0$ (which is linear, and can be solved analytically, thereby bypassing otherwise severe stability restrictions).

It can be shown (Suzuki, [41]) that methods of orders above two will need to feature at least some negative time increments. Although this is of little concern in our context of Maxwell’s equations, it does make the splitting idea problematic in cases when an equation is partly dissipative, such as for example the Navier-Stokes equations.

To heuristically explain why splitting works, we can for simplicity replace (11) by $u_t = Au + Bu$ where A and B are constant matrices (the procedure allows for more general nonlinear operators, but in our present context of Maxwell’s equations, A and B will become matrices after we have discretized in space). In this simplified case we can write the analytic solution of the system (11) of ODEs as

| Method | Time increment | sequence |
|--------|---|--|
| SS1 | 0.50000 00000 00000 00000 | 0.50000 00000 00000 00000 |
| SS2 | 0.25000 00000 00000 00000 | 0.50000 00000 00000 00000 0.25000 00000 00000 00000 |
| SS4 | 0.33780 17979 89914 40851 -0.85120 71919 59657 63405 0.33780 17979 89914 40851 | 0.67560 35959 79828 81702 -0.08780 17979 89914 40851 0.67560 35959 79828 81702 |
| SS6 | 0.19612 84026 19389 31595 0.11778 66066 79679 06684 0.03437 65841 26260 05298 -0.58883 99920 89435 50347 0.25502 17059 59228 84938 | 0.39225 68052 38778 63191 -0.23552 66927 04878 21832 0.25502 17059 59228 84938 -0.23552 66927 04878 21832 0.11778 66066 79679 06684 0.65759 31603 41955 60944 0.03437 65841 26260 05298 -0.23552 66927 04878 21832 0.19612 84026 19389 31595 |
| SS8 | 0.22871 10615 57447 89169 0.12684 66682 83105 67707 -0.40077 32180 57163 83322 0.96906 95688 11262 99329 -0.46445 25958 95878 59173 0.85422 65353 93640 79233 -0.46445 25958 95878 59173 0.96906 95688 11262 99329 -0.40077 32180 57163 83322 0.12684 66682 83105 67707 0.22871 10615 57447 89169 | 0.45742 21231 14895 78337 -0.29778 97250 73598 45089 0.29213 43956 99000 73022 -0.29778 97250 73598 45089 -0.72242 61184 30302 57885 0.44497 46255 63618 95284 0.44497 46255 63618 95284 -0.00561 77738 38196 20526 -0.98030 51164 87655 40380 0.05139 99246 95898 22035 0.45281 32300 44769 50634 0.45281 32300 44769 50634 0.05139 99246 95898 22035 -0.98030 51164 87655 40380 -0.00561 77738 38196 20526 0.44497 46255 63618 95284 -0.07912 03176 84025 08760 -0.72242 61184 30302 57885 -0.29778 97250 73598 45089 0.29213 43956 99000 73022 0.45742 21231 14895 78337 |

Table 1. Coefficients of some Split-Step methods

$$u(t) = e^{(A+B)t} u(0)$$

where $e^{(A+B)t}$ is to be understood as the matrix

$$\begin{aligned} e^{(A+B)t} &= I + t(A + B) + \frac{t^2}{2!}(A + B)^2 + \dots \\ &= I + t(A + B) + \frac{t^2}{2!}(A^2 + AB + BA + B^2) + \dots \end{aligned} \tag{12}$$

(taking note of the fact that A and B in general do not commute). The solution operator using SS1 amounts to replacing the exact operator $e^{(A+B)t}$ by

$$\begin{aligned} e^{2B\frac{t}{2}} e^{2A\frac{t}{2}} &= (I + tB + \frac{t^2}{2!}B^2 + \dots)(I + tA + \frac{t^2}{2!}A^2 + \dots) \\ &= I + t(A + B) + \frac{t^2}{2!}(A^2 + 2BA + B^2) + \dots \end{aligned} \tag{13}$$

The expansion in (13) differs from the one in (12) in the t^2 -term. This tells that this particular splitting is only first order accurate. Carrying out the same expansion for the SS2 scheme gives

$$\begin{aligned} e^{2A\frac{t}{4}} e^{2B\frac{t}{2}} e^{2A\frac{t}{4}} &= (I + \frac{t}{2}A + \frac{t^2}{8}A^2 + \dots)(I + tB + \frac{t^2}{2}B^2 + \dots)(I + \frac{t}{2}A + \frac{t^2}{8}A^2 + \dots) \\ &= I + t(A + B) + \frac{t^2}{2!}(A^2 + AB + BA + B^2) + \dots \end{aligned}$$

This agrees with (12) throughout the t^2 -term, thereby ensuring that SS2 (Strang splitting) indeed is accurate to second order.

A similar verification in the case of SS4 will produce an expansion that reproduces (12) also through the next two powers of t (not displayed in (12)). This SS4 scheme was originally found (via direct algebraic expansions similar to the ones above) by Neri in 1987 [34]. Closed form expressions are in this case available for the fractional step lengths c_i and d_i in the expansion

$$e^{(A+B)t} = e^{c_1 A t} e^{d_1 B t} e^{c_2 A t} e^{d_2 B t} e^{c_3 A t} e^{d_3 B t} e^{c_4 A t} + O(t^5),$$

namely

$$c_1 = c_4 = \frac{1}{2(2 - 2^{1/3})}, \quad c_2 = c_3 = (1 - 2^{1/3})c_1, \quad d_1 = d_3 = 2c_1, \quad d_2 = -2^{4/3}c_1.$$

The key contributions by Yoshida in 1990 [45] were to

- demonstrate that it is possible to find sequences of time increments that give time stepping accuracies of any order;
- devise a practical algorithm for computing these sequences of increments; and
- note that, in order to get a high order in time, special time step sequences can be applied as an addition to any scheme that is second order accurate (i.e. if we have any second order scheme for (7) – irrespective of if it is itself based on splitting or not – we can use certain time stepping sequences to bring it up to any order in time). This will be discussed later.

A couple of comments regarding the last point above.

- We can use either ADI or CNS (Strang split 3D Maxwell's equations, using Crank-Nicolson for the sub-problems – as will be described next) as our basic scheme, and then use certain time step sequences to enhance it to higher orders. This will become one of the three enhancement techniques we will consider later for increasing the time accuracy of the unconditionally stable ADI and CNS schemes.
- The methods SS4, SS6, SS8 in Table 1 are just special cases of this more general observation. These schemes arise if we choose, as our basic second order scheme in this process the CNS scheme (here also denoted SS2).

Application of Split Step to Maxwell's Equations Immediate dimensional splitting of the 3D Maxwell's equations would lead us to consider a PDE of the form $\frac{\partial \underline{u}}{\partial t} = A\underline{u} + B\underline{u} + C\underline{u}$ where \underline{u} denotes the vector $(E_x, E_y, E_z, H_x, H_y, H_z)^T$. Although 3-way splitting is feasible, the particular structure of the 3D Maxwell's equations permits a much more effective alternative. We start this by writing the Maxwell's equations as we did earlier in (7) and, like then, we abbreviate them as

$$\frac{\partial \underline{u}}{\partial t} = A\underline{u} + B\underline{u} \tag{14}$$

The split-step approach leads us to repeatedly advance $\frac{\partial \underline{u}}{\partial t} = 2A\underline{u}$ and $\frac{\partial \underline{u}}{\partial t} = 2B\underline{u}$ by certain time increments. These two subproblems can be written out explicitly as shown below. As first noted by Lee and Fornberg [29], each of the two subproblems obtained in this manner amount to three pairs of mutually entirely uncoupled 1D equations:

$$\left\{ \begin{array}{l} \left\{ \begin{array}{l} \frac{\partial E_x}{\partial t} = \frac{2}{\varepsilon} \frac{\partial H_z}{\partial y} \\ \frac{\partial H_z}{\partial t} = \frac{2}{\mu} \frac{\partial E_x}{\partial y} \end{array} \right\} \\ \left\{ \begin{array}{l} \frac{\partial E_y}{\partial t} = \frac{2}{\varepsilon} \frac{\partial H_x}{\partial z} \\ \frac{\partial H_x}{\partial t} = \frac{2}{\mu} \frac{\partial E_y}{\partial z} \end{array} \right\} \\ \left\{ \begin{array}{l} \frac{\partial E_z}{\partial t} = \frac{2}{\varepsilon} \frac{\partial H_y}{\partial x} \\ \frac{\partial H_y}{\partial t} = \frac{2}{\mu} \frac{\partial E_z}{\partial x} \end{array} \right\} \end{array} \right\}, \quad \left\{ \begin{array}{l} \left\{ \begin{array}{l} \frac{\partial E_x}{\partial t} = -\frac{2}{\varepsilon} \frac{\partial H_y}{\partial z} \\ \frac{\partial H_y}{\partial t} = -\frac{2}{\mu} \frac{\partial E_x}{\partial z} \end{array} \right\} \\ \left\{ \begin{array}{l} \frac{\partial E_y}{\partial t} = -\frac{2}{\varepsilon} \frac{\partial H_z}{\partial x} \\ \frac{\partial H_z}{\partial t} = -\frac{2}{\mu} \frac{\partial E_y}{\partial x} \end{array} \right\} \\ \left\{ \begin{array}{l} \frac{\partial E_z}{\partial t} = -\frac{2}{\varepsilon} \frac{\partial H_x}{\partial y} \\ \frac{\partial H_x}{\partial t} = -\frac{2}{\mu} \frac{\partial E_z}{\partial y} \end{array} \right\} \end{array} \right\}. \quad (15)$$

Each of the 1D subsystems in (15) can very easily be solved numerically. If we choose a method which preserves the L^2 -norm for each 1D sub-problem, the sum of the squares of all the unknowns will be preserved through each sub-step, and therefore also throughout the complete computation. Unconditional numerical stability is then assured. In particular, this will be the case if we approximate each of the 1D subsystems in (15) with a Crank-Nicolson type approximation. For example, to advance the first of the six sub-problems a distance $\Delta t/4$ in time, we would use

$$\frac{E_x|_{i,j,k}^{n+1/4} - E_x|_{i,j,k}^n}{\Delta t/4} = \frac{2}{\varepsilon} \frac{1}{2} \left\{ \frac{H_z|_{i,j+1,k}^{n+1/4} - H_z|_{i,j-1,k}^{n+1/4}}{2\Delta y} + \frac{H_z|_{i,j+1,k}^n - H_z|_{i,j-1,k}^n}{2\Delta y} \right\}$$

$$\frac{H_z|_{i,j,k}^{n+1/4} - H_z|_{i,j,k}^n}{\Delta t/4} = \frac{2}{\mu} \frac{1}{2} \left\{ \frac{E_x|_{i,j+1,k}^{n+1/4} - E_x|_{i,j-1,k}^{n+1/4}}{2\Delta y} + \frac{E_x|_{i,j+1,k}^n - E_x|_{i,j-1,k}^n}{2\Delta y} \right\}$$

If we here use the second equation to eliminate H_z on the new time level from the first equation, we get a tridiagonal system to solve for E_x . Advancing (14) using Strang splitting together with these Crank-Nicolson approximations gives the scheme that we denote by CNS, which is second order accurate in time and space.

Comparison Between Different Split Step Sequences The possibility of using split step together with (15) for numerical time integration of Maxwell's equations was first explored in [29]. In that study, a periodic domain was used, and all the 1D subproblems were solved analytically in (discrete) Fourier space. All errors that arose were therefore due to the time stepping, and it became possible to clearly compare the effectiveness of SS schemes of different orders. One of the observations that was made there was that different split step methods of the same order can have very different leading error coefficients. Seven different SS8 methods have been found.

Fig. 10 shows, for a typical test problem, how the accuracy improves with increased temporal resolution. In this log-log plot, the slopes of the curves confirm the 8th order of accuracy in all cases, but the errors nevertheless differ by a full $3\frac{1}{2}$ orders of magnitude (for details about the test, see the original paper). The scheme that performs the best here – SS8d – is the one given in Table 1. Simply looking at the coefficients for the different schemes gives no clear indication of their difference in accuracy.

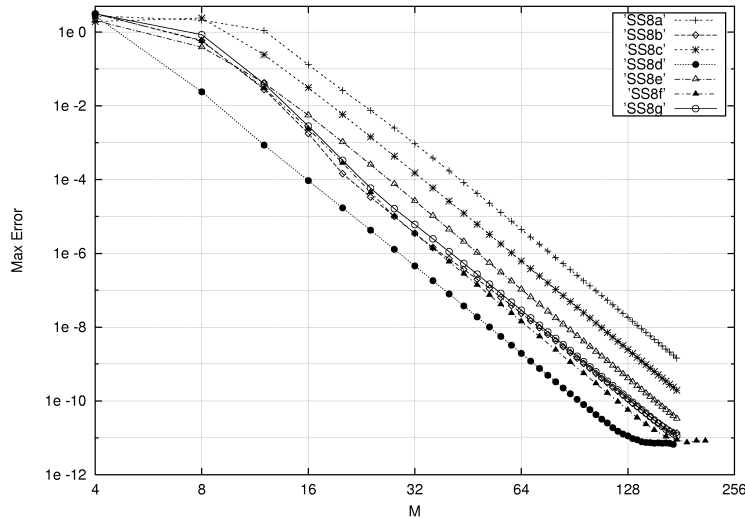


Fig. 10. Log-log plot comparison of error vs. number of subintervals in time for seven different SS8 methods

4.3 Enhancements to Reach Higher Orders of Accuracy in Time

We have just described two possible ways to obtain second order accuracy in time combined with unconditional stability (at least for pure initial value problems): ADI and CNS. High order methods are usually more effective than low order ones. In the present case of space being over-resolved (with respect to the wave length – in order to capture the fine geometrical features), we are in the (unusual) situation that it is not important to bring up the spatial order of accuracy. The situation in time is fundamentally different. Only one scale is present – a large one imposed by the wave length. A high order time stepping method can give cost savings by means of allowing significantly

longer time steps than can be used with a second order method – as long as the unconditional stability is preserved.

Some approaches to reach higher order in time are certain *not* to work. For example, explicit Runge–Kutta and linear multistep methods can never feature unbounded stability domains. Because of the second Dahlquist stability barrier [2, 3] there are no prospects either in trying to add more back time levels to the ADI scheme; no implicit linear multistep method can combine A -stability with higher than second order accuracy in time. Following the treatment in Lee and Fornberg [30], we will next discuss three enhancements to ADI and CNS that will reach higher orders in time without running into the difficulties just mentioned. As it will transpire, two of them (later to be denoted EX and DC) will preserve unconditional stability up to all orders, at least for pure initial value problems in the case of constant media (the only situation for which stability has been rigorously established for the ADI and CNS methods). It appears that the third approach (TS) will preserve stability up to fourth order, but strong evidence for this is still lacking. For orders higher than four, cases of instability have been found. We will next introduce the three approaches (in the order TS, EX and DC).

Special Time–Step Sequences The pioneering paper – as well as the main reference – on this procedure is Yoshida [45]. We start by assuming that we have some numerical procedure which advances our solution with second order accuracy in time. Expressed in the form of an operator, we write the advancement of the solution from time t to the time $t + \tau$ as $\underline{u}(t + \tau) = S_2(\tau) \underline{u}(t)$. We furthermore assume that the local error in the $S_2(\tau)$ –operator is expandable in terms of the time step τ in the form $c_1\tau^3 + c_2\tau^5 + c_3\tau^7 + \dots$. It then transpires that the composite operator

$$S_4(\tau) = S_2(w_1\tau) S_2(w_0\tau) S_2(w_1\tau) \tag{16}$$

becomes (globally) fourth order accurate in time if the constants w_0 and w_1 are chosen as $w_0 = -\frac{2^{1/3}}{2-2^{1/3}}$ and $w_1 = \frac{1}{2-2^{1/3}}$. This idea can be continued indefinitely, with the general result stating that

$$S_{2p}(\tau) = S_2(w_k\tau) \dots S_2(w_1\tau) S_2(w_0\tau) S_2(w_1\tau) \dots S_2(w_k\tau)$$

is accurate of order $2p$ if the constants $w_k, k = 0, 1, \dots, 2^{p-1} - 1$ satisfy certain nonlinear systems of algebraic equations. For the $p = 2$ case the system becomes

$$\begin{cases} w_0 + 2w_1 = 1 \\ w_0^3 + 2w_1^3 = 0 \end{cases} \tag{17}$$

and in case of $p = 3$

| Order (2p) | Coefficients w_0, w_1, \dots, w_k where $k = 2^{p-1} - 1$. |
|---------------|---|
| 4 | - 1.70241 43839 19315 26810 1.35120 71919 59657 63405 |
| 6 | 1.31518 63206 83911 21888 - 1.17767 99841 78871 00695 0.23557 32133 59358 13368 0.78451 36104 77557 26382 |
| 8 | 1.70845 30707 87281 58467 0.10279 98493 91796 44070 - 1.96061 02329 75310 80761 1.93813 91376 22525 98658 -0.15824 06353 68050 17520 -1.44485 22368 60605 15769 0.25369 33365 66211 35415 0.91484 42462 29791 56675 |

Table 2. Coefficients of some time increment sequences

$$\left\{ \begin{array}{l} w_0 + 2(w_1 + w_2 + w_3) = 1 \\ w_0^3 + 2(w_1^3 + w_2^3 + w_3^3) = 0 \\ w_0^5 + 2(w_1^5 + w_2^5 + w_3^5) = 0 \\ -w_0^4 w_1 - w_0^3 w_1^2 + w_0^2 w_1^3 + w_0 w_1^4 - w_0^4 w_2 - 2w_0^3 w_1 w_2 - 2w_0^2 w_1^2 w_2 - 4w_0^4 w_3 - w_0^3 w_2^2 - 2w_0^3 w_2^2 + \\ + w_0^2 w_2^3 + 4w_0 w_1 w_2^2 + 4w_1^2 w_2^2 + w_0 w_2^3 + 2w_1 w_2^3 - w_0^3 w_3 - 2w_0^2 w_1 w_3 - 2w_0 w_1^2 w_3 - 4w_1^3 w_3 - \\ - 2w_0^3 w_2 w_3 - 4w_1^3 w_2 w_3 - 2w_0 w_2^3 w_3 - 4w_1 w_2^3 w_3 - 4w_2^4 w_3 - w_0^3 w_3^2 - 2w_0^3 w_3^2 - 2w_0^3 w_3^2 + w_0^2 w_3^3 + \\ + 4w_0 w_1 w_3^2 + 4w_1^2 w_3^2 + 4w_0 w_2 w_3^2 + 8w_1 w_2 w_3^2 + 4w_2^2 w_3^2 + w_0 w_3^4 + 2w_1 w_3^4 + 2w_2 w_3^4 = 0 \end{array} \right. \quad (18)$$

Convenient recursive expressions to create the algebraic system for the general order of accuracy $2p$ are given in [45]. These are very well suited for numerical computation of the coefficients. Since the number of steps in these time-step sequences increase exponentially with the order, fairly low orders are probably of most interest. Table 2 will therefore suffice for most needs.

If we apply these sequences to the SS2 method, we get the methods we earlier described as SS4, SS6, etc. But the sequences can just as well be applied to other second order time stepping methods, such as the ADI method. In the following, we will sometimes denote the original ADI method as ADI2, and the time sequence enhancements of it as ADI-TS4, ADI-TS6, etc.

Table 2 gives one example of coefficients for each order. The eighth order scheme that is listed here corresponds to the split step scheme that was most effective in the comparison shown in Fig. 10. Coefficients for all presently known schemes up to and including 8^{th} order can be found in [29].

We conclude this section by briefly explaining how the systems (17), (18) etc. can be obtained. If X and Y are operators (or matrices) that commute, then $e^X \cdot e^Y = e^Z$ with $Z = X + Y$. If X and Y do not commute, the expression for Z becomes far more complicated. By the Baker-Campbell-Hausdorff (BCH) formula [43]

$$\begin{aligned} Z = & (X + Y) + [X, Y] \\ & + \frac{1}{12} ([X, X, Y] + [Y, Y, X]) \\ & + \frac{1}{24} [X, Y, Y, X] \\ & + \left\{ \begin{array}{l} \text{commutators of successi-} \\ \text{vely increasing orders} \end{array} \right\} \end{aligned} \quad (19)$$

where $[X, Y] = XY - YX$, $[X, Y, V] = [X, [Y, V]]$, etc. Repeated application of (19) gives $e^X \cdot e^Y \cdot e^X = e^W$ where

$$W = (2X + Y) + \frac{1}{6} ([Y, Y, X] - [X, X, Y]) + \left\{ \begin{array}{l} \text{commutators of successi-} \\ \text{vely increasing orders} \end{array} \right\} \quad (20)$$

With our assumption that the operator $S_2(\tau)$ advances the equation $u' = Au$ the distance τ in time, with a local error of $c_1\tau^3 + c_2\tau^5 + \dots$, it can be written as $S_2(\tau) = e^{\tau A + \tau^3 C + O(\tau^5)}$. The RHS of (16) then becomes

$$e^{\overbrace{(w_1\tau)A + (w_1\tau)^3 C + O(\tau^5)}^X} e^{\overbrace{(w_0\tau)A + (w_0\tau)^3 C + O(\tau^5)}^Y} e^{\overbrace{(w_1\tau)A + (w_1\tau)^3 C + O(\tau^5)}^X}$$

By (20) this becomes

$$e^{\overbrace{(2w_1 + w_0)\tau A + (2w_1^3 + w_0^3)\tau^3 C + O(\tau^5)}^{2X+Y}} + \overbrace{O(\tau^5)}^{\text{higher terms}}$$

This represents a fourth order method if it is of the form $e^{\tau A + O(\tau^5)}$, i.e. if (17) holds. To reach higher orders, we need to extend (20) to products of still more exponentials. When the commutators also come into play for some of the relations that need to be satisfied, the complexity of the resulting algebraic equations rapidly increases, as is seen in (18). However, as we noted just above, the original reference [45] shows that the higher order systems can nevertheless be obtained recursively very conveniently.

For some further developments on 'composition methods' for time stepping, see Hairer et al. [24].

Richardson Extrapolation The idea, going back to Lewis Fry Richardson in 1927 [37], has been used since then in many applications, e.g. in extrapolation methods for ODEs and as Romberg's method for quadrature. If we have a numerical procedure for which the error of a computed variable u depends on a step size h in the following way

$$u_h = \text{Exact} + c_1 h^2 + c_2 h^4 + \dots,$$

then repeating this calculation using a step size $h/2$ will give

$$u_{h/2} = \text{Exact} + c_1 \frac{1}{4} h^2 + c_2 \frac{1}{16} h^4 + \dots$$

These two results can be linearly combined in order to eliminate $c_1 h^2$, giving the more accurate result

$$v_{h/2} = \frac{4 u_{h/2} - u_h}{3} = \text{Exact} - c_2 \frac{1}{4} h^4 + \dots$$

This idea can be continued repeatedly, and the results are conveniently laid out in triangular form

| Directly computed | Extrapolated | | |
|----------------------|--|--|--|
| order 2 | order 4 | order 6 | order 8 |
| u_h | | | |
| $u_{h/2}$ | $v_{h/2} = \frac{4u_{h/2} - u_h}{3}$ | | |
| $u_{h/4}$ | $v_{h/4} = \frac{4u_{h/4} - u_{h/2}}{3}$ | $w_{h/4} = \frac{16v_{h/4} - v_{h/2}}{15}$ | |
| $u_{h/8}$ | $v_{h/8} = \frac{4u_{h/8} - u_{h/4}}{3}$ | $w_{h/8} = \frac{16v_{h/8} - v_{h/4}}{15}$ | $x_{h/8} = \frac{64w_{h/8} - w_{h/4}}{63}$ |
| ... | ... | ... | ... |

In the context of quadrature, it is common practice to halve the step between each calculation (in order to be able to re-use as many old function values as possible). The drawback with that strategy is that the number of function evaluations then grows exponentially with the order. In the context of ODEs – which is our situation when time stepping Maxwell’s equations – it is cheaper to make smaller changes in the time step between the different computations. The extrapolation procedure will still increase the order by two for each new original computation, but without the need for each new computation to be twice as expensive as the previous one.

Deferred Correction This concept of deferred correction was introduced by Pereyra [36], first in the context of solving 2-point boundary value problems for ODEs, and subsequently for solving PDEs. Frank and collaborators [17–19] use the method for increasing the order of accuracy in the time stepping of ODEs. This was considered again recently by Gustafsson and Kress [23] who also illustrate the effectiveness of this for a methods-of-lines solution of a 1D heat equation. We will describe it here in the context of the ADI scheme. The procedure to increase the temporal order of accuracy from 2 to 4 consists of the following steps.

- Run the ADI2 scheme over some time interval $[0, T]$.
- From the numerical values of this solution, evaluate an approximation of the local truncation error $\underline{E}^{n+1/2}$ at each time level.
- Re-run the ADI2 scheme over the time $[0, T]$, but this time include $\underline{E}^{n+1/2}$ as a RHS (a forcing function) to the equation.

The last two steps can be repeated in order to reach still higher orders of accuracy (6, 8, etc.). Two orders of accuracy will be gained each time the basic second order scheme is re-run.

To apply this idea to the ADI scheme, we start by noting that the local error in (9) becomes

$$\begin{aligned} \underline{E}^{n+1/2} &= \left(1 - \frac{\Delta t}{2}A\right) \left(1 - \frac{\Delta t}{2}B\right) \underline{u}^{n+1} - \left(1 + \frac{\Delta t}{2}A\right) \left(1 + \frac{\Delta t}{2}B\right) \underline{u}^n \\ &= \left(1 + \frac{(\Delta t)^2}{4}AB\right) (\underline{u}^{n+1} - \underline{u}^n) - \frac{\Delta t}{2} (\underline{u}^{n+1} + \underline{u}^n) \end{aligned}$$

From the expansions

$$\begin{aligned}\underline{u}^{n+1} - \underline{u}^n &= \Delta t \underline{u}_t^{n+1/2} + \frac{(\Delta t)^3}{24} \underline{u}_{ttt}^{n+1/2} + \frac{(\Delta t)^5}{1920} \underline{u}_{ttttt}^{n+1/2} + \dots \\ \underline{u}^{n+1} + \underline{u}^n &= 2\underline{u}^{n+1/2} + \frac{(\Delta t)^2}{4} \underline{u}_{tt}^{n+1/2} + \frac{(\Delta t)^4}{192} \underline{u}_{tttt}^{n+1/2} + \dots\end{aligned}$$

follow

$$\begin{aligned}\underline{E}^{n+1/2} &= (\Delta t) \left(\underline{u}_t^{n+1/2} - (A+B)\underline{u}^{n+1/2} \right) + && \text{Vanishes because of the PDE} \\ &+ (\Delta t)^3 \left(\frac{AB}{4} \underline{u}_t^{n+1/2} - \frac{A+B}{8} \underline{u}_{tt}^{n+1/2} + \frac{1}{24} \underline{u}_{ttt}^{n+1/2} \right) + && \text{Use to get DC of order 4} \\ &+ (\Delta t)^5 \left(\frac{AB}{96} \underline{u}_{ttt}^{n+1/2} - \frac{A+B}{384} \underline{u}_{tttt}^{n+1/2} + \frac{1}{1920} \underline{u}_{ttttt}^{n+1/2} \right) + && \text{Use to get DC of order 6} \\ &+ \dots && \dots\end{aligned}$$

To proceed from ADI2 to ADI-DC4 (deferred correction to 4th order), we approximate $\underline{E}^{n+1/2}$ by

$$\begin{aligned}\underline{E}^{n+1/2} &\approx \frac{(\Delta t)^2}{4} AB (\underline{u}^{n+1} - \underline{u}^n) - \frac{\Delta t}{16} (A+B) (\underline{u}^{n+2} - \underline{u}^{n+1} - \underline{u}^n + \underline{u}^{n-1}) \\ &+ \frac{1}{4} (\underline{u}^{n+2} - 3\underline{u}^{n+1} + 3\underline{u}^n - \underline{u}^{n-1}).\end{aligned}$$

In the same manner as we showed that (9) was equivalent to (10), we can show that

$$\left(1 - \frac{\Delta t}{2}A\right) \left(1 - \frac{\Delta t}{2}B\right) \underline{u}^{n+1} = \left(1 + \frac{\Delta t}{2}A\right) \left(1 + \frac{\Delta t}{2}B\right) \underline{u}^n + \underline{E}^{n+1/2} \quad (21)$$

is equivalent to

$$\begin{cases} \left(1 - \frac{\Delta t}{2}A\right) \underline{u}^{n+1/2} = \left(1 + \frac{\Delta t}{2}B\right) \underline{u}^n + \frac{1}{2}\underline{E}^{n+1/2} \\ \left(1 - \frac{\Delta t}{2}B\right) \underline{u}^{n+1} = \left(1 + \frac{\Delta t}{2}A\right) \underline{u}^{n+1/2} + \frac{1}{2}\underline{E}^{n+1/2}. \end{cases} \quad (22)$$

Multiplying the second equation in (22) by $\left(1 - \frac{\Delta t}{2}A\right)$ and then using the first equation in (22) leads in a few steps to (21)

$$\begin{aligned}\left(1 - \frac{\Delta t}{2}A\right) \left(1 - \frac{\Delta t}{2}B\right) \underline{u}^{n+1} &= \left(1 - \frac{\Delta t}{2}A\right) \left(1 + \frac{\Delta t}{2}A\right) \underline{u}^{n+1/2} + \frac{1}{2} \left(1 - \frac{\Delta t}{2}A\right) \underline{E}^{n+1/2} \\ &= \left(1 + \frac{\Delta t}{2}A\right) \left(1 - \frac{\Delta t}{2}A\right) \underline{u}^{n+1/2} + \frac{1}{2} \left(1 - \frac{\Delta t}{2}A\right) \underline{E}^{n+1/2} \\ &= \left(1 + \frac{\Delta t}{2}A\right) \left\{ \left(1 + \frac{\Delta t}{2}B\right) \underline{u}^n + \frac{1}{2}\underline{E}^{n+1/2} \right\} + \frac{1}{2} \left(1 - \frac{\Delta t}{2}A\right) \underline{E}^{n+1/2} \\ &= \left(1 + \frac{\Delta t}{2}A\right) \left(1 + \frac{\Delta t}{2}B\right) \underline{u}^n + \underline{E}^{n+1/2}.\end{aligned}$$

The corrections in this deferred correction procedure can therefore be very conveniently implemented by applying half the amount of the approximative local error to each of the two ADI stages.

Enhancements by Re-starts During computations over long times, *re-starts* can improve the accuracy of both Richardson extrapolation and deferred correction calculations. Instead of running the calculations over $[0, T]$, we run at first over $[0, T/2]$ to obtain an accurate value at $T/2$. Then, re-starting from that point, we compute up to time T . This amounts to a ‘2 subinterval’ calculation. A ‘4 subinterval’ calculation would similarly split $[0, T]$ into $[0, T/4]$, $[T/4, T/2]$, $[T/2, 3T/4]$, $[3T/4, T]$, etc. The idea is to avoid ever running the underlying low-order method across a long time interval, as it would then accumulate very large errors. Subsequent extrapolation or deferred correction would then have little chance of working well. With the re-start approach, the low-order computations will never be given the time to drift too far off course, and the subsequent corrections will therefore be correspondingly more effective. For additional discussion and test results, see [30].

Abbreviations for the Time Stepping Methods The time stepping methods we have just introduced and which we next will compare are

| | |
|---------|---|
| ADI | Alternating Direction Implicit FDTD method |
| CNS | Split step method of order 2 using Crank-Nicolson |
| ADI-TS | Time sequence enhanced ADI |
| CNS-TS | Time sequence enhanced CNS |
| ADI-EX | Richardson extrapolation enhanced ADI |
| ADI-DC | Deferred correction enhanced ADI |
| ADI-REX | The ADI-EX method further enhanced by restarts |
| ADI-RDC | The ADI-DC method further enhanced by restarts |

Since it was found in [30] that the ADI-based methods might be marginally more effective than the CNS-based ones, we will here not include CNS-EX, CNS-DC, CNS-REX and CNS-RDC. At the end of each of the abbreviations, we also add a number specifying the order in time.

Test Problem We consider the following exact periodic solution to (1) over the unit cube with $\varepsilon = \mu = 1$:

$$\begin{aligned} E_x &= \cos(2\pi(x + y + z) - 2\sqrt{3}\pi t) & H_x &= \sqrt{3}E_x \\ E_y &= -2E_x & H_y &= 0 \\ E_z &= E_x & H_z &= -\sqrt{3}E_x. \end{aligned} \quad (23)$$

We discretize all spatial derivatives by centered second order finite differences. Instead of quoting the size of the time and space steps explicitly, we instead give *points per time interval* (PPT, number of time steps / total time T for test problem) and *points per wave length* (PPW, with the wave length

here equal to $\sqrt{3}$). By converting the spatial variables over to the Fourier domain, the system to be solved can be written as $\hat{u}_t = A\hat{u}$ where A is a 6×6 matrix (independently of how fine we choose our spatial discretization). On this new system of ODEs, we then carry out all our different time stepping procedures. This conversion over to the Fourier domain allows us to observe the influence of the PPW quantity also for very high values without this leading to any increased computational cost per time step.

Computational Cost Comparisons Fig. 11 illustrates how the L_2 error at a final time $t = 1$ varies with PPW and PPT. The value of PPW determines the spatial discretization error level. If PPW is held fixed and PPT is increased without bound, time stepping errors will decrease to zero, and the total error will come down to the level that is set by the spatial errors for the particular value of PPW. In the limit of $PPW = \infty$ we will only see time stepping errors. The errors for the different methods will then decrease indefinitely, as is indicated by the dotted extrapolations in Fig. 12 (near to where we have labeled the different methods).

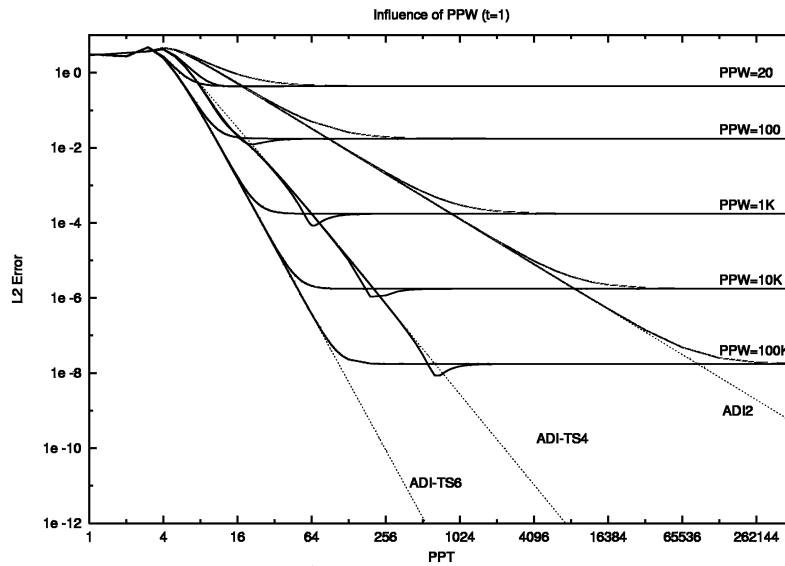


Fig. 11. L_2 error at time $t = 1$ as function of PPW and PPT in the case of the ADI method and time-sequence enhanced versions of it

In Fig. 12 we have fixed PPW to 10^5 , but have also indicated in the right margin what the asymptotic error levels becomes for other PPW choices. Again, extrapolations corresponding to $PPW = \infty$ are also shown. When comparing the relative computational cost between different time stepping

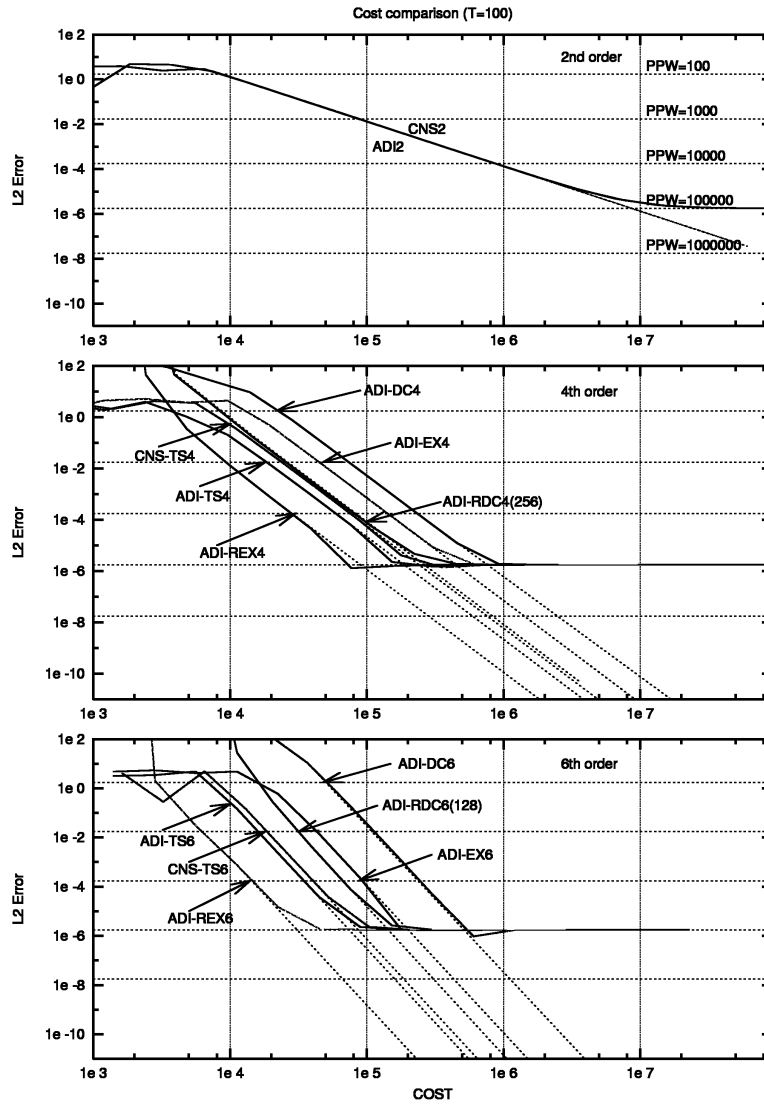


Fig. 12. L_2 error at time $T = 100$ as function of PPW and of relative computational cost for time stepping methods of different orders

methods, we need to consider not only the number of time steps but also the number of operations per time step. The three subplots show the errors for our time stepping methods of orders 2, 4, and 6 respectively, when this

cost has been factored in – thus with relative cost replacing PPT along the horizontal axis. We can make a number of observations from Fig. 12.

- Unless PPW is quite large, there is little reason to increase the order in time beyond what ADI2 offers.
- For very high PPW (the situation in the class of problems we are considering; with geometrical features much smaller than a typical wave length), the benefits of higher order time stepping can be substantial.
- Of the three different enhancement approaches, DC (deferred correction) appears the least effective and EX (Richardson extrapolation) the most effective.

The situation with regard to unconditional stability is somewhat unclear in the case of the TS methods. It appears to hold for TS4 but, in certain cases, does not hold for TS6. For the DC and EX methods, it will hold for all orders as long as the number of restarts are held finite (rather than being increased with PPT). Re-started, high order extrapolations of the ADI approach (ADI-REX) appears to be particularly attractive for high PPW calculations.

For more details on these higher order enhancements (such as how the number of re-starts influence the resulting accuracy), see Lee and Fornberg [30]. In conclusion, regarding this class of time stepping methods, it needs to be added that they so far have been applied only to very simple periodic problems. Tests with variable media and irregular interfaces should be carried out before any firm recommendations can be made.

4.4 Conclusions

Problems in CEM feature two length scales: the size of geometric features, and a typical wave length. The first part of this article focused on the case when the length scales are similar. Thanks to its simplicity, the Yee scheme has been popular in many applications. Its drawbacks are its low (second order) accuracy and lack of geometric flexibility. We noted that it can be enhanced to high orders in both space and time by using wider FD stencils and by incorporating more back levels respectively. The novel, high-order time-staggered linear multistep methods that were briefly described have better stability and accuracy properties than their classical Adams-type non-staggered counterparts. The difficulty with geometric flexibility can be met by taking a hybrid approach, such as switching to a FE scheme near interfaces or to a FD scheme on ‘patches’ that are mapped to follow curved interfaces. Boundary integral methods can in some cases give very high efficiency, not only for time harmonic cases but also for fully time dependent ones.

After mentioning a few implementations, we turned our attention to cases where the geometrical features are many orders of magnitude smaller than a typical wave length. The primary issue then becomes how to effectively bypass the CFL stability condition. Two second order accurate methods with

unconditional stability have recently been found, ADI and CNS. The remainder of the paper has been devoted to a description of these and a discussion about how they can be enhanced to feature higher order accuracies in time (without losing their unconditional stability). Mixed with reports of successful implementations and insights are also some tentative concerns, e.g. the

- significance of the lack of exact pointwise conservation of $\text{div}(\varepsilon E)$ and $\text{div}(\mu H)$ is unclear;
- possibility of large errors arising from the $\frac{(\Delta t)^2}{4} A B(\underline{u}^{n+1} - \underline{u}^n)$ term in (8) in cases of variable coefficients (and which constant media dispersion analysis does not seem to reveal [21]);
- stability situation with regard to ADI-type methods in combination with certain boundary conditions;
- accuracy of some of the high order time stepping approaches in cases when the equations have explicit time dependence due to the boundary conditions or to forcing.

All these issues are at present under study by different research groups. These open questions notwithstanding, ADI-type methods form an exciting new direction in CEM, now on the verge of moving from test problems to production applications.

4.5 Acknowledgements

Several of the results described here have been obtained in collaboration with Toby Driscoll and Jongwoo Lee. In addition, very helpful discussions with Fredrik Edelvik, Jan Hesthaven, and Gunnar Ledfelt are gratefully acknowledged.

References

1. O. Bruno, New high-order, high-frequency methods in computational electromagnetism, Topics in Computational Wave Propagation 2002, Springer (2003).
2. G. Dahlquist, Convergence and stability in the numerical integration of ordinary differential equations, Math. Scand. 4 (1956), 33–53.
3. G. Dahlquist, 33 years of numerical instability, part I, BIT, 25 (1985), 188–204.
4. M. Darms, R. Schuhmann, H. Spachmann and T. Weiland, Asymmetry effects in the ADI-FDTD algorithm, to appear in IEEE Microwave Guided Wave Lett.
5. L. Demkowicz, Fully automatic hp-adaptive finite elements for the time-harmonic Maxwell's equations, Topics in Computational Wave Propagation 2002, Springer (2003).
6. J. Douglas, Jr, On the numerical integration of $\frac{\partial^2 u}{\partial x^2} + \frac{\partial^2 u}{\partial y^2} = \frac{\partial u}{\partial t}$ by implicit methods, J. Soc. Indust. Appl. Math., 3 (1955), 42–65.
7. T.A. Driscoll and B. Fornberg, Block pseudospectral methods for Maxwell's equations: II. Two-dimensional, discontinuous-coefficient case, SIAM Sci. Comput. 21 (1999), 1146–1167.

8. F. Edelvik and G. Ledfelt, A comparison of time-domain hybrid solvers for complex scattering problems, *Int. J. Numer. Model* 15 (5–6) (2002), 475–487.
9. M. El Hachemi, Hybrid methods for solving electromagnetic scattering problems on overlapping grids, in preparation.
10. E. Forest and R.D. Ruth, Fourth order symplectic integration, *Physica D* 43 (1990), 105–117.
11. B. Fornberg, *A Practical Guide to Pseudospectral Methods*, Cambridge University Press (1996).
12. B. Fornberg, Calculation of weights in finite difference formulas, *SIAM Review*, 40 (1998), 685–691.
13. B. Fornberg, A short proof of the unconditional stability of the ADI-FDTD scheme, University of Colorado, Department of Applied Mathematics Technical Report 472 (2001).
14. B. Fornberg, High order finite differences and the pseudospectral method on staggered grids, *SIAM J. Numer. Anal.* 27(1990), 904–918.
15. B. Fornberg and T.A. Driscoll, A fast spectral algorithm for nonlinear wave equations with linear dispersion, *JCP*, 155 (1999), 456–467.
16. B. Fornberg and M. Ghrist, Spatial finite difference approximations for wave-type equations, *SIAM J. Numer. Anal.* 37 (1999), 105–130.
17. R. Frank and C.W. Ueberhuber, Iterated defect correction for differential-equations 1. Theoretical results, *Computing*, 20 Nr 3 (1978), 207–228.
18. R. Frank, F. Macsek and C.W. Ueberhuber, Iterated defect correction for differential-equations 2. Numerical experiments, *Computing*, 33 Nr 2 (1984), 107–129.
19. R. Frank, J. Hertling and H. Lehner, Defect correction algorithms for stiff ordinary differential equations, *Computing*, Supplement 5 (1984), 33–41.
20. L. Gao, B. Zhang and D. Liang, Stability and convergence analysis of the ADI-FDTD algorithm for 3D Maxwell equation. In preparation.
21. S.G. García, T.-W. Lee and S.C. Hagness, On the accuracy of the ADI-FDTD method, *IEEE Antennas and Wireless Propagation Letters* 1 No 1 (2002), 31–34.
22. M. Ghrist, T.A. Driscoll and B. Fornberg, Staggered time integrators for wave equations, *SIAM J. Num. Anal.* 38 (2000), 718–741.
23. B. Gustafsson and W. Kress, Deferred correction methods for initial value problems, *BIT* 41 (2001), 986–995.
24. E. Hairer, C. Lubich and G. Wanner, *Geometric Numerical Integration*, Springer Verlag (2002).
25. J. Hesthaven and T. Warburton, Nodal high-order methods on unstructured grids I. Time-domain solution of Maxwell's equations, *JCP*, 181 (2002), 186–221.
26. R. Hiptmair, Finite elements in computational electromagnetism, *Acta Numerica* 2002 (2002), 237–339.
27. J. Jin, *The Finite Element Method in Electromagnetics*, Wiley, New York (1993).
28. K.S. Kunz and J. Luebbers, *The Finite Difference Time Domain Method for Electromagnetics*, CRC Press, Inc. (1993).
29. J. Lee and B. Fornberg, A split step approach for the 3D Maxwell's equations, University of Colorado, Department of Applied Mathematics Technical Report 471 (2001), submitted to *Journal of Computational and Applied Mathematics* (2002).

30. J. Lee and B. Fornberg, Some unconditionally stable time stepping methods for the 3D Maxwell's equations, Submitted to IMA journal of Applied Mathematics (2002).
31. G. Liu and S.D. Gedney, Perfectly matched layer media for an unconditionally stable three-dimensional ADI-FDTD method, *IEEE Microwave Guided Wave Lett.* 10 (2000), 261–263.
32. J.C. Maxwell, *A Treatise on Electricity and Magnetism*, Clarendon Press, Oxford (1873).
33. T. Namiki, 3D ADI-FDTD method – Unconditionally stable time-domain algorithm for solving full vector Maxwell's equations, *IEEE Transactions on Microwave Theory and Techniques*, 48, No 10 (2000), 1743–1748.
34. F. Neri, Lie algebras and canonical integration, Dept. of Physics, University of Maryland, preprint (1987).
35. D. Peaceman and J.H.H. Rachford, The numerical solution of parabolic and elliptic differential equations, *J. Soc. Indust. Appl. Math.* 3 (1955), 28–41.
36. V. Pereyra, Accelerating the convergence of discretization algorithms, *SIAM J. Numer. Anal.* 4 (1967), 508–532.
37. L.F. Richardson, The deferred approach to the limit, *Phil. Trans. A*, 226 (1927), 299–349.
38. T. Rylander and A. Bondeson, Stable FEM-FDTD hybrid method for Maxwell's equations, *Computer Physics Communications*, 125 (2000), 75–82.
39. B. Shanker, A.A. Ergin, K. Aygun, E. Michielssen, Analysis of transient electromagnetic scattering phenomena using a two-level plane wave time-domain algorithm, *IEEE Trans. Antennas Propagation* 48 (2000), 510–523.
40. G. Strang, On construction and comparison of difference schemes, *SIAM J. Numer. Anal.* 5 (1968), 506–516.
41. M. Suzuki, General theory of fractal path integrals with applications to many-body theories and statistical physics, *J. Math. Phys.* 32 (1991), 400–407.
42. A. Taflove and S.C. Hagness, *Computational Electrodynamics: The Finite-Difference Time-Domain Method*, 2nd ed., Artech House, Norwood (2000).
43. V.S. Varadarajan, *Lie groups, Lie algebras and their representation*, Prentice Hall, Englewood Cliffs (1974).
44. K.S. Yee, Numerical solution of initial boundary value problems involving Maxwell's equations in isotropic media, *IEEE Trans. Antennas Propagation*, 14 (1966), 302–307.
45. H. Yoshida, Construction of higher order symplectic integrators, *Physics Letters A*, 150 (1990), 262–268.
46. F. Zheng, Z. Chen, J. Zhang, A finite-difference time-domain method without the Courant stability conditions, *IEEE Microwave Guided Wave Lett.* 9 (1999), 441–443.
47. F. Zheng, Z. Chen, J. Zhang, Toward the development of a three-dimensional unconditionally stable finite-difference time-domain method, *IEEE Transactions on Microwave Theory and Techniques*, 48, No 9 (2000), 1550–1558.